

Optical and infrared observations of the Type II SN 2002hh from day 3 to 397

M. Pozzo¹, W.P.S. Meikle¹, J.T. Rayner², R.D. Joseph², A.V. Filippenko³,
R.J. Foley³, W. Li³, S. Mattila⁴, J. Sollerman^{4,5}

¹ *Imperial College London, Blackett Laboratory, Prince Consort Road, London, SW7 2BW, U.K.*

² *Institute for Astronomy, University of Hawaii, 2680 Woodlawn Drive, Honolulu, HI 96822*

³ *Department of Astronomy, 601 Campbell Hall, University of California, Berkeley, CA 94720-3411*

⁴ *Stockholm Observatory, AlbaNova, Dept. of Astronomy, Stockholm SE 106 91, Sweden*

⁵ *DARK cosmology center, NBI, Copenhagen University, Denmark*

Accepted ... Received ; in original form 2004 ...

ABSTRACT

We present optical and infrared (IR) observations of the type II SN 2002hh from day 3 to 397 days after explosion. The optical spectroscopic (4–397 d) and photometric (3–278 d) observations are complemented by spectroscopic (137–381 d) and photometric (137–314 d) data acquired at IR wavelengths. This is the first time L-band spectroscopic observations have ever been successfully achieved for a supernova at a distance beyond the Local Group. The *VRI* light curves in the first 40 days type SN 2002hh as a SN IIP - the most common of all core-collapse supernovae. SN 2002hh is one of the most highly-extinguished supernovae ever investigated. To provide a match between its early-time spectrum and a coeval spectrum of the Type IIP SN 1999em as well as maintaining consistency with K I interstellar absorption, we invoke a 2-component extinction model. One component is due to the combined effect of the interstellar medium (ISM) of our galaxy and the SN host galaxy while the other component is due to a “dust pocket” where the grains have a mean size smaller than in the ISM. The early-time optical light curves of SNe 1999em and 2002hh are generally well-matched, as are the radioactive tails of these two SNe and SN 1987A. The late-time similarity of the SN 2002hh optical light curves to those of SN 1987A, together with measurements of the *OIR* luminosity and [Fe II] 1.257 μm emission indicate that $(0.07 \pm 0.02) M_{\odot}$ of ^{56}Ni was ejected by SN 2002hh. However, during the nebular phase the *HKL'* luminosities of SN 2002hh exhibit a growing excess with respect to those of SN 1987A. We attribute much of this excess to an IR-echo from a pre-existing, dusty circumstellar medium (CSM). Based on an IR-echo interpretation of the near-IR (NIR) excess we deduce that the progenitor of SN 2002hh underwent a recent mass-loss of $\sim 0.3 M_{\odot}$. A detailed comparison of the late time optical and NIR spectra of SNe 1987A and 2002hh is presented. While the overall impression is one of similarity between the spectra of the two events, there are notable differences. The Mg I 1.503 μm luminosity of SN 2002hh is $\times 2.5$ greater than in SN 1987A at similar epochs, yet coeval silicon and calcium lines in SN 2002hh are fainter. Interpreting these differences as being due to abundance variations, the overall abundance trend between SN 1987A and SN 2002hh is not consistent with explosion model predictions. It appears that during the burning to intermediate-mass elements, the nucleosynthesis did not progress as far as might have been expected given the mass of iron ejected. Evidence for mixing in the ejecta is presented. Pronounced blueshifts are seen in the more isolated lines and these are attributed to asymmetry in the ejecta. However, during the timespan of these observations (~ 1 year post-explosion) we find no evidence of dust condensation in the ejecta such as might have been revealed by an increasing blueshift and/or attenuation of the red wings of the emission lines. Nevertheless, the clear detection of first overtone CO emission by 200 days and the reddening trend in $(K - L')_0$ suggest that dust formation in the ejecta may occur at later epochs. From the [O I] 6300,6364 \AA doublet luminosity we infer a 16–18 M_{\odot} main-sequence progenitor star. The progenitor of SN 2002hh was probably a red supergiant with a substantial, dusty wind.

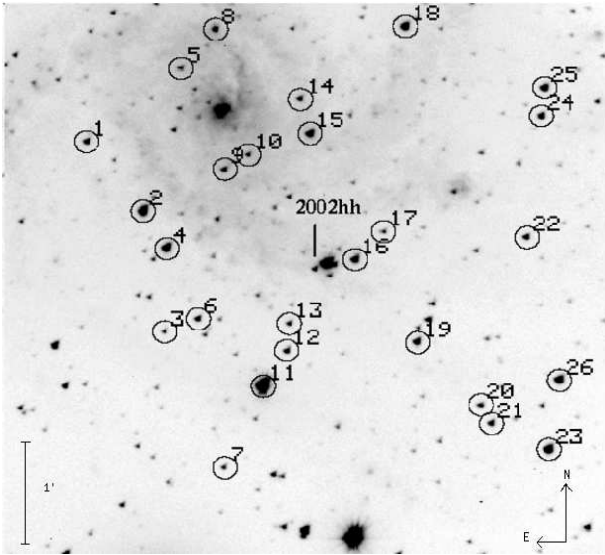


Figure 1. R-band image of the SN 2002hh field taken with KAIT on 2002 December 2 UT, when the SN was about one month post-explosion. The nucleus of the host galaxy, NGC 6946, is visible at the top-left corner. Also shown are the local standards used for the photometric calibration (see Table 1).

1 INTRODUCTION

An important goal of astrophysics is to deepen our understanding of the progenitors and explosion mechanisms of core-collapse supernovae (CCSNe). What kind of stars explode? What drives the explosion? Do CCSNe or their progenitors contribute significant quantities of dust to the ISM? Observations of CCSNe at late times have a unique potential for helping us to answer these questions since by these epochs, i.e. the *nebular phase* ($t > 150$ d), we can view directly most of the ejecta. This allows measurements of element/molecule abundances and distributions such as was achieved for SN 1987A (e.g. Meikle et al. 1989, 1993; Varani et al. 1990; Spyromilio, Meikle & Allen 1990; Spyromilio et al. 1991). The drawback is that by the time the nebular phase is reached the supernova has become faint. Consequently only the very nearest events can be effectively studied in this way. An excellent opportunity for the study of the nebular phase came with the discovery of SN 2002hh which is one of the nearest type II SN in the past 50 years. Type II supernovae make up the most common subgroup of CCSNe. SN 2002hh was very highly reddened with a V-band extinction which reduced its flux by a factor of $> \times 100$. However, the effect of the extinction is much reduced in the infrared and indeed it can be argued (see below) that this wavelength region is at least as important as the optical region for late-time studies.

IR observations can test the nature of CCSNe in ways which are not available in other wavelength regions. Constraints on the CCSN progenitor can be obtained with a combination of IR/optical photometry and IR spectroscopy. For example, the presence of first overtone CO emission (*K*-band) in CCSNe is increasingly regarded as ubiquitous, having been detected in all seven CCSNe which have been

observed in the *K*-band at 3-6 months post-explosion (see Gerardy et al. 2002 and refs. therein; Meikle et al. 2003 and refs. therein). By modelling the first overtone CO spectrum of the Type II_n SN 1998S Fassia et al. (2001) deduced a CO mass of $10^{-3} M_{\odot}$, while from the bolometric light curve they deduced a mass of $0.15 M_{\odot} {}^{56}\text{Ni}$. Combining these two results they inferred a core mass exceeding $4 M_{\odot}$, implying a massive progenitor. In addition, the detection of CO is important since it is probably an essential precursor to dust condensation in the ejecta.

Infrared spectroscopy during the photospheric phase can probe ejecta-mixing and hence the explosion mechanism. Graham (1988) showed how the strong He I 1.083 μm line at early times could be used to infer the upward mixing of radioactive iron-group elements in the ejecta of the peculiar Type II SN 1987A. Fassia et al. (1998) and Fassia & Meikle (1999) developed further this technique and applied it, respectively, to the Type IIP SN 1995V and to the peculiar Type II SN 1987A.

In spite of the high extinction toward SN 2002hh, optical spectra are also of value. The prominent, high S/N H α and Ca II lines allow investigation of ejecta asymmetry. The fluoresced 8446 \AA O I line provides confirmation of the identification of the O I 1.1287 μm line, and the cascade pair together may allow us to study the conditions under which such lines are formed (Spyromilio et al. 1991).

A major goal in the study of CCSNe is to provide a significant test of the proposal that they are, or have been, a significant source of dust in the universe. While this hypothesis is over 30 years old (Cernuschi, Marsicano & Codina, 1967; Hoyle & Wickramasinghe, 1970) and is still popular (Gehrz, 1989; Tielens 1990; Dwek 1998; Todini & Ferrara 2001; Nozawa et al., 2003) *direct evidence that SNe are major dust sources is still very sparse*. Indeed, it is not known if ordinary Type II SNe or their progenitors produce large amounts of dust at all. Dust condensation in CCSN ejecta can be detected in two ways. In one method, we can make use of the infrared emission from the hot dust grains. 13 CCSNe (cf. Gerardy et al., 2002 and refs. therein), plus 1 peculiar Type Ia event (SN 2002ic: Kotak et al., 2004) have shown a strong, late-time NIR excess implying the presence of hot dust. However, it is difficult to establish whether this dust was newly-condensed in the metal-rich SN ejecta or existed previously in the progenitor's wind and was detected via an IR-echo. Even the comprehensive multi-epoch NIR study of the Type II_n SN 1998S by Pozzo et al. (2004) could not resolve completely this ambiguity. While their favoured interpretation was that at least $10^{-3} M_{\odot}$ of dust formed in the cool dense shell at the ejecta/CSM interface, the alternative IR-echo interpretation was not ruled out. Dunne et al. (2003) claimed that their sub-mm observations of the SN remnant Cassiopeia A indicates that $>1 M_{\odot}$ of dust formed in the ejecta, but this has been recently disproved by Krause et al. (2004) as being instead due to interstellar dust in a molecular cloud complex located in the line of sight between the Earth and Cas A. The other way of detecting newly-condensed dust is via its attenuating effect on the red wings of the broad ejecta lines during the nebular phase. This technique has the advantage of being relatively unambiguous in

its ability to demonstrate the presence of new dust, although it may be more difficult to extract quantitative information about the quantity and nature of the grains. However, owing to the difficulty of acquiring high-quality spectra at late-times, this method has demonstrated ejecta dust in just three cases so far: the type IIpec SN 1987A, (Danziger et al. 1991; Lucy et al. 1991), the type IIP SN 1999em (Elmhamdi et al. 2003) and the type IIin SN 1998S (Pozzo et al. 2004). Thus, the close proximity of SN 2002hh offers us only the second-ever opportunity for the study of dust condensation in the most common type of CCSNe.

SN 2002hh was discovered on UT 2002 October 31.1 (UT dates are used throughout this paper) during the course of the Lick Observatory Supernova Search (LOSS; Li et al. 2000; Filippenko et al. 2001) with the 0.76-m Katzman Automatic Imaging Telescope (KAIT) (Li 2002). It was discovered at about 16.5 mag (see Fig. 1) and peaked at $V \sim +15$ mag in mid-November. SN 2002hh was not detected on a previous KAIT image taken on October 26.1 at a limiting magnitude of ~ 19.0 . We shall therefore adopt 2002 October 29 as the explosion epoch, the uncertainty being about ± 2 days. SN 2002hh occurred in NGC 6946, an Scd galaxy which has produced 7 other SNe. Five of these other events were typed: SNe 1917A (II), 1948B (IIP), 1968D (II), 1980K (IIL) and 2004et (IIP) while SNe 1939C and 1969P were untyped. SN 2002hh is located at R.A. = 20h34m44s.29, Decl. = $+60^\circ 07' 19''.0$ (2000.0) which is $60''.9$ west and $114''.1$ south of the nucleus (Li 2002). We adopt a host galaxy distance of 5.9 ± 0.4 Mpc (Karachentsev, Sharina & Huchtmeier 2000). Spectra taken by Filippenko, Foley & Swift (2002) on 2002 November 2 revealed broad, very low-contrast H α emission and absorption lines, but with a nearly featureless and very red continuum (cf. Fig. 6). Strong, narrow (interstellar) Na I D absorption is also present. Filippenko et al. inferred a very young, highly-reddened Type II supernova. The high reddening was confirmed and measured by Meikle et al. (2002) on Nov. 18.86 UT from IR images. Adopting a phase of 21 days, comparison of the $J - K_s$ colour with the infrared-template light curves of Mattila & Meikle (2001) indicated $E(J - K_s) = 1.0$. From the reddening law of Cardelli, Clayton & Mathis (1989), this yields $A_V \sim 6.1$ mag. Subtracting the Galactic extinction (Schlegel, Finkbeiner & Davis 1998) leads to a host-galaxy extinction A_V of ~ 5.0 mag. For a distance of 5.9 Mpc, Meikle et al. (2002) derived de-reddened absolute IR magnitudes of $M(J) = -18.3$ and $M(K_s) = -18.5$, which are close to the values given by the templates of Mattila & Meikle (2001) for normal type II supernovae. We note that SN 2004et occurred in the same galaxy as SN 2002hh, but was not highly reddened (Li et al. 2005a). We attribute this to the fact that SN 2004et occurred in a “clean” region at the edge of the galaxy while SN 2002hh is located on a spiral arm. SN 1917A also occurred in NGC 6946, just $\sim 22''.0$ from SN 2002hh, but has no measured extinction.

Stockdale et al. (2002) reported detection of radio emission from the supernova with the VLA at 17 d (Nov. 15.25 UT) and confirmed the previously reported optical position. They measured fluxes of (0.60 ± 0.10) mJy at 22.485 GHz and (0.81 ± 0.08) mJy at 8.435 GHz. From the apparently optically thin character of the radio emission, they suggest

that the circumstellar interaction was weak at this epoch, and was evolving unusually rapidly. Pooley & Lewin (2002) reported the detection of X-ray emission from SN 2002hh with the Chandra X-ray observatory at 27 d confirming the previously reported optical and radio positions. The low X-ray luminosity detected is consistent with the weak circumstellar interaction indicated by the radio observations. Preliminary spectral fits to the X-ray data indicate a column density of $N_H = 10^{22} \text{ cm}^{-2}$. SN 2002hh was also detected at 1396.75 MHz with the Giant Meterwave Radio Telescope at 59 d (undetected at 32 d) (Chandra, Ray & Bhatnagar 2003). More recently, Beswick et al. (2005) reported VLA measurements of (0.35 ± 0.1) mJy at 4.860 GHz on day 381 and (1.6 ± 0.2) mJy at 1.425 GHz on day 899.

Barlow et al. (2005) reported the detection of SN 2002hh in archival Spitzer Space Telescope images (obtained in the SINGS Legacy Program) covering $3.6\text{--}24 \mu\text{m}$, in June and November 2004 as well as in an $11.2 \mu\text{m}$ Gemini/Michelle image taken in September 2004. They report a 25 per cent decline in the total $8 \mu\text{m}$ flux between days 590 and 758 and suggest that most of the mid-IR emission originates in a massive ($10\text{--}15 M_\odot$), dusty circumstellar shell (i.e., an IR-echo). They also propose that a large fraction of the extinction is due to this circumstellar dust. However, they do not rule out the possibility that a small fraction of the mid-IR emission may have originated in newly-formed dust in the ejecta. In contrast, but on the basis of the same data, Meikle et al. (2005a,b and in prep.) find a decline of just 4 per cent in the $8 \mu\text{m}$ flux between days 590 and 758. They conclude that to produce such a large and slowly-declining flux with an IR echo would require a CSM mass of at least $10 M_\odot$ assuming a normal dust/gas ratio. However, they find only a small amount of the extinction should be attributed to this dust. They suggest that most of the mid-IR flux could be foreground/background emission and that only the small declining component originates in the supernova. They propose that this could be consistent with radiation from warm, newly-condensed dust having a mass comparable to that seen in SN 1987A *viz.* $10^{-3} M_\odot$. More recent Spitzer observations (Meikle et al. in prep.) show a similarly slow rate of decline between days 758 and 996 as that obtained by Meikle et al. at earlier phases. For the echo hypothesis, this pushes the required CSM mass even higher and so argues even more strongly against most of the mid-IR flux arising in an IR echo. The apparent disagreement between the two sets of authors is not yet resolved.

In this paper we describe our IR and optical photometric and spectroscopic observations of SN 2002hh from day 3 to 397. The paper is organized as follows. Optical/IR imaging and spectroscopic observations and data reduction are presented in Section II. In this Section, we also present VRI lightcurves of SN 2002hh together with IR light curves and colour curves. Section III deals with redshift and extinction. In particular, we show that the high extinction towards the SN is best described with a 2-component extinction model with different grain sizes. We also derive the OIR luminosity of the SN and the mass of ejected ^{56}Ni . Section IV is devoted to the analysis of the spectroscopic behaviour and the main elements detected in the optical and IR spectra. In Section V we compare SN 2002hh with the well-studied core-collapse SN 1987A. Their optical and IR spectra at coeval epochs, al-

Table 1. Photometry of the comparison stars for SN 2002hh.

ID	V	R	I
1	15.47(1) ^a	14.98(1)	14.46(1)
2	13.57(0)	13.14(2)	12.79(3)
3	16.86(2)	16.30(1)	15.74(2)
4	13.78(1)	13.34(1)	12.95(3)
5	16.97(3)	16.45(1)	15.94(2)
6	15.80(2)	15.32(1)	14.83(2)
7	16.67(2)	16.14(1)	15.56(2)
8	15.94(2)	15.28(1)	14.64(1)
9	16.16(2)	15.59(1)	15.05(1)
10	16.75(2)	16.18(1)	15.60(1)
11 ^b	12.32(3)	11.84(2)	11.88(3)
12	15.82(2)	15.37(2)	14.88(2)
13	16.41(2)	15.75(1)	15.12(1)
14	16.38(1)	15.83(1)	15.28(1)
15	15.06(1)	14.17(1)	13.36(1)
16	14.74(2)	14.27(2)	13.81(3)
17	16.90(3)	16.45(3)	15.96(2)
18	14.81(1)	14.14(1)	13.48(2)
19	14.85(2)	14.35(2)	13.88(2)
20	16.85(2)	16.00(1)	15.32(1)
21	15.48(2)	15.00(0)	14.53(1)
22	15.67(2)	15.22(1)	14.75(0)
23	13.84(1)	13.36(1)	12.93(3)
24	15.63(2)	14.93(1)	14.36(1)
25	14.46(1)	14.02(1)	13.59(1)
26	14.38(2)	13.70(0)	13.10(2)

^a Figures in brackets give the internal error, in units of the magnitude's least significant digit.

^b This local field star was saturated in many frames and therefore was not used for the final photometric calibration.

though similar, show some interesting differences. The evolution of the CO emission and the unidentified 2.265 μm feature originally detected in SN 1987A are also discussed. Finally, the late-time near-IR continuum and the temporal evolution of the extinction-corrected $(K - L')_0$ colour for SN 2002hh are analyzed. Conclusions follow in Section VI.

2 OBSERVATIONS

2.1 Optical photometry

We obtained *VRI* images of SN 2002hh during the first ~ 300 days post-explosion with KAIT. An Apogee AP7 512 \times 512 SITE CCD camera was used, covering a total field-of-view of 6'.7 \times 6'.7 at 0.8 arcsec/pixel. The images were reduced using standard IRAF^{*} routines. PSF-fitting photometry was performed after galaxy subtractions using *VRI* template images of the SN field acquired on 2004 Aug 19 UT after the supernova had faded away (a recent unfiltered image of the field with exceptional seeing showed that the SN might be fainter than 20 mag). Local stars in the field of the host galaxy (see

^{*} IRAF (Image Reduction and Analysis Facility) is distributed by the National Optical Astronomy Observatory (NOAO), which is operated by the Association of Universities for Research in Astronomy (AURA), Inc. under cooperative agreement with the National Science Foundation.

Table 2. *VRI* photometry of SN 2002hh.

JD(2450000+)	Epoch ^a	V	R	I
2580.60	3	17.30(7) ^b	15.64(7)	14.31(6)
2581.62	4	17.28(4)	15.60(3)	14.27(3)
2583.60	6	17.18(5)	15.53(5)	14.19(5)
2590.62	13	17.29(3)	15.60(3)	14.29(6)
2594.65	17	17.20(6)	15.57(3)	14.24(3)
2596.61	19	17.29(6)	15.60(6)	14.26(6)
2605.62	28	17.32(5)	15.55(3)	14.26(4)
2610.59	33	17.48(4)	15.65(4)	14.31(4)
2620.62	43	17.45(4)	15.67(3)	14.23(4)
2744.01	166	19.53(16)	17.40(7)	16.01(8)
2757.01	180	19.71(13)	17.53(6)	16.09(7)
2765.97	188	19.52(10)	17.56(5)	16.18(6)
2774.89	197	–	17.45(8)	15.96(7)
2783.98	206	19.85(16)	17.53(5)	16.08(5)
2792.96	216	19.78(13)	17.85(6)	16.33(6)
2801.94	224	20.16(16)	17.89(5)	16.52(5)
2819.91	242	20.36(19)	18.08(5)	16.61(4)
2828.88	250	20.09(21)	17.91(6)	16.62(5)
2837.92	260	20.74(35)	18.17(6)	16.85(3)
2846.80	269	20.25(25)	18.25(7)	17.01(7)
2855.81	278	–	18.64(5)	16.93(5)

^a Days after explosion, assumed to be 2002 October 29 UT (JD 2452577.5).

^b Figures in brackets give the internal error, in units of the magnitude's least significant one or two digits.

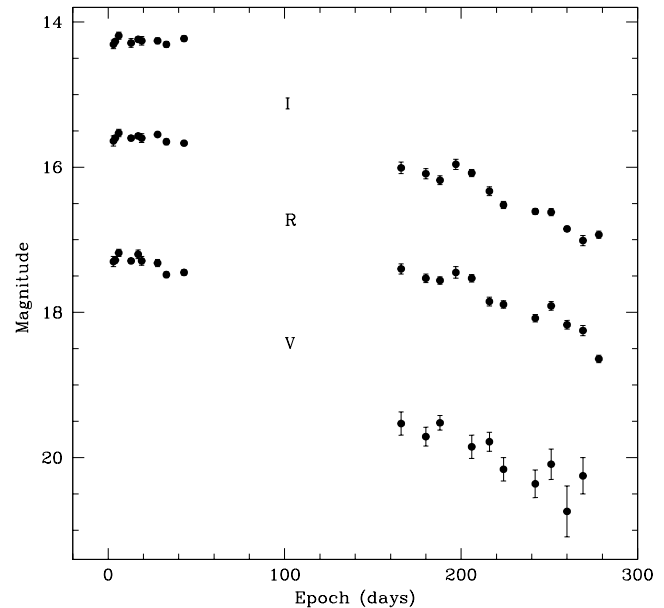
**Figure 2.** *VRI* lightcurves of SN 2002hh.

Fig. 1 and Table 1) were measured on three different dates (2002 Nov 5 UT, 2003 May 31 UT, and 2003 Jun 1 UT), calibrated against many fields (some 10 to 15) of Landolt standard stars observed at different airmasses at each night (for a final RMS solution of about 0.01 mag in all the filters) and finally used for the photometric calibration of the SN magnitudes. The error in the photometry was estimated by

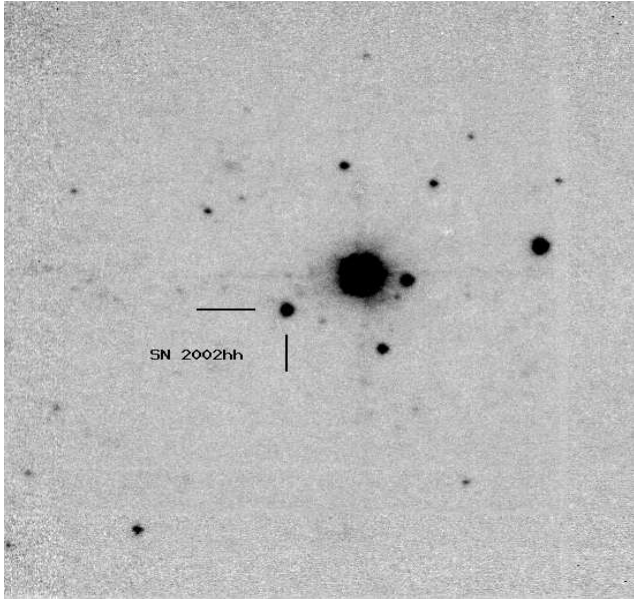


Figure 3. K-band image of SN 2002hh taken with the SpeX imager on 2003 July 22, when the SN was about nine months post-explosion.

adding in quadrature the RMS of the transformed magnitude of the SN from the observed local standard stars and the error in the IRAF PSF-fitting. As such, the resulting error is an underestimate of the real uncertainty (not taking into account, for example, the error caused by the quality of the galaxy subtraction technique). Final optical VRI magnitudes and associated errors are listed in Table 2, while the corresponding light curves are shown in Fig. 2. The temporal evolution of the VRI magnitudes during the first 40 d shows a typical plateau phase, which types SN 2002hh as a type IIP SN, the most common supernova type (see also Fig. 13). The late-time decline rates in the VRI bands were roughly linear at about 0.007, 0.011 and 0.008 mag/day respectively and of the same order of those found in the IR bands (see below).

2.2 Near-infrared photometry

The SpeX imager at IRTF (see Section 2.4) was used to obtain *JHKL'* images of SN 2002hh at four epochs between days 137 and 314. These epochs correspond to four of the five epochs when NIR spectroscopy was also obtained (see below). The imager employs an Aladdin 2 512×512 InSb array covering a 60'0×60'0 field-of-view at 0.12 arcsec/pixel. A standard imaging procedure was performed, using 5- to 10-point jitter patterns. The images were reduced using standard IRAF routines. The jittered on-source exposures were median combined to form sky frames in the *JHK* bands for both the supernova and the standard stars. In the *L'*-band, where the sky varies rapidly, sky subtraction was performed by subtracting consecutive pairs of on-source offset exposures from each other. In each band, the sky-subtracted frames were then median-combined. Fig. 3 shows the K-band image of SN 2002hh taken with the SpeX imager on 2003

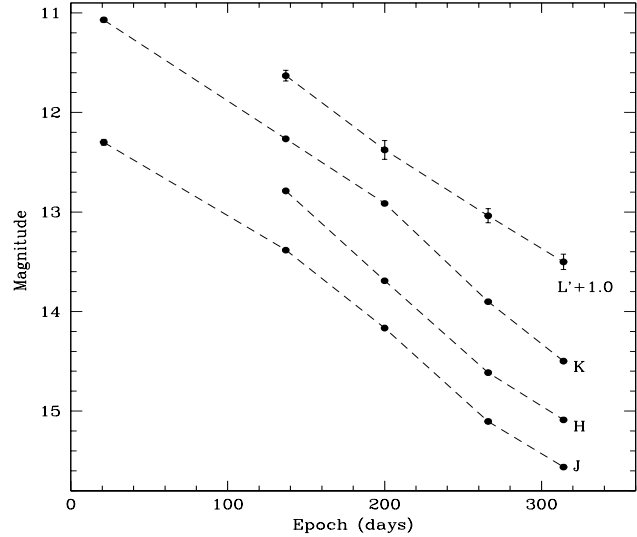


Figure 4. *JHKL'* light curves of SN 2002hh. Also shown there are the the early (+21 d) J and K points. Only the statistical errors are shown (see text).

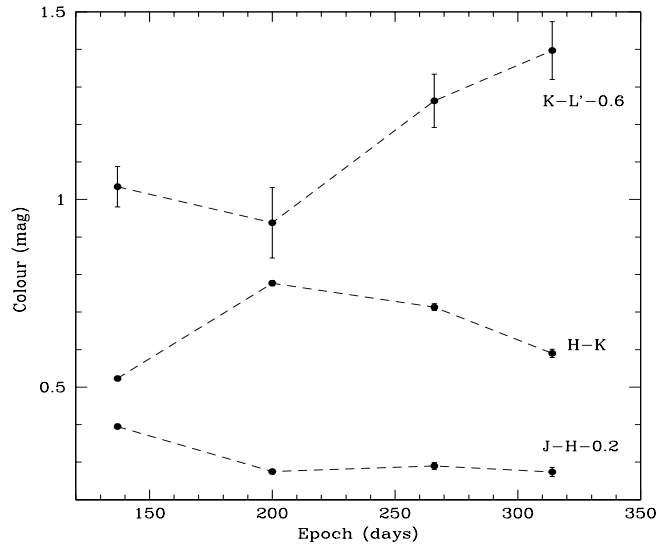


Figure 5. Post-100 d IR colour evolution of SN 2002hh. Only the statistical errors are shown (see text).

July 22, when the SN was about nine months post-explosion.

Aperture photometry was carried out within the Starlink package GAIA[†] (Draper, Gray & Berry 2002) using an aperture radius equivalent to $\times 2.5$ FWHM of the standard star PSF viz. 18 pixels, equivalent to 2'16. The sky background was measured using a concentric annular aperture, with inner and outer radii respectively of $\times 1.5$ and $\times 2.5$ that of the aperture (see Pozzo et al. 2004 for details). The sky variance with 2 sigma clipping was used to determine the photometric statistical uncertainty. Table 3 lists the details of the IR imaging observations, including the standard stars

[†] Graphical Astronomy and Image Analysis Tool, version 2.6-9

Table 3. Log of IR photometric observations taken at IRTF with SpeX.

JD(245 0000+)	Date (2003)	Epoch ^a	Photometric standard	Observers
2714.5	Mar 15	137	FS150 (JHK), HD203856 (L')	R.D. Joseph, J.T. Rayner
2777.5	May 17	200 ^b	HD201941 (JHKL') ^c	J.T. Rayner
2843.5	Jul 22	266	FS150 (JHK), HD201941 (L')	R.D. Joseph, J.T. Rayner
2891.5	Sep 8	314	FS150 (JHK), HD201941 (L')	J.T. Rayner

^a Days after explosion.^b Mostly cloudy, this night was non-photometric.^c Due to the non-photometric night, this standard star was not used for calibration; see text for details.**Table 4.** IR photometry and colours of SN 2002hh.

JD(2450000+)	Epoch ^a	J	H	K	L'	J-H	H-K	K-L'
2714.5	137	13.383(1) ^b	12.788(1)	12.265(1)	10.631(54)	0.595(1)	0.523(1)	1.634(54)
2777.5	200	14.166(3)	13.691(4)	12.914(6)	11.376(94)	0.475(5)	0.777(7)	1.538(94)
2843.5	266	15.104(6)	14.614(7)	13.901(6)	12.038(71)	0.490(9)	0.713(9)	1.863(71)
2891.5	314	15.562(7)	15.088(10)	14.498(4)	12.501(77)	0.474(12)	0.590(11)	1.997(77)

^a Days after explosion.^b Figures in brackets give the internal error, in units of the magnitude's least significant one or two digits.

used. On most nights the magnitudes were determined directly by comparison with the standards observed on the same nights. However, the 200 d epoch was clearly non-photometric and so on this occasion calibrations was carried out via relative photometry of SN field stars.

The resulting IR magnitudes and colours of SN 2002hh are listed in Table 4 and plotted in Figs. 4 and 5. Associated statistical errors are shown in parentheses and as error bars. The late-time decline rates in the JHKL' bands were roughly linear at, respectively, about 0.012, 0.013, 0.013 and 0.011 mag/day. The J-H and H-K colours remained roughly constant at ~ 0.5 and ~ 0.7 respectively during the 137–314 d period. The K-L' colour reddened between days 137 and 314 from about 1.6 to about 2.0 mag.

2.3 Optical spectroscopy

Optical spectra were obtained at 8 epochs spanning 4–397 days post-explosion. We used: the Kast double spectrograph (Miller & Stone 1993) mounted on the Lick Observatory 3.0 m Shane telescope on Mt. Hamilton; the Echellette Spectrograph and Imager (ESI; Sheinis et al. 2002) mounted on the 10.0 m Keck II telescope on Mauna Kea; the ISIS spectrograph at the 4.2m William Herschel Telescope (WHT) and the ALFOSC spectrograph at the 2.56 m Nordic Optical Telescope (NOT), both on La Palma; and the Low Resolution Imaging Spectrometer (LRIS; Oke et al. 1995) mounted on the 10.0 m Keck I telescope on Mauna Kea.

With the Lick/Kast we used the 452/3306 Grism and the 300/7500 Grating, together with 180x1200 and 210x1200 CCD arrays, each having a 0.798 arcsec/pixel scale. With the Keck/ESI we used the 175 lines/mm grating and 32.3 degree blaze grisms, with a 2048x4096 CCD array having a 0.12-0.17 arcsec/pixel scale. With the WHT/ISIS we used the R316R grating and the EEV4290 MARCONI2 detector

with a 0.20 arcsec/pixel scale. With the NOT/ALFOSC we used Grism 5 (0.5-1.025 μm) and the Loral 2048x2048 array (CCD7, now retired) with a 0.19 arcsec/pixel scale. With Keck/LRIS we used the 400/3400 Grism and the 400/8500 Grating equipped with the 4620x4096 and 1000x2245 CCD arrays respectively, having a 0.211 and 0.135 arcsec/pixel scale each. For the Kast, ESI, ISIS and LRIS spectra the position angle of the slit was generally aligned along the parallactic angle to reduce differential light losses (Filippenko 1982). For the NOT spectrum, the slit was positioned at PA 181° in order to minimise contamination from the bright nearby star (2MASS J20344320+6007234) lying about 9'0 WNW from the supernova. Table 5 gives details of the optical spectroscopic observations. Standard stars used are also listed, together with slit widths and position angles.

The spectra from Kast, ESI and LRIS were reduced using standard techniques as described by Li et al. (2001) and references therein. Flatfields for the red CCD were taken at the position of the object to reduce NIR fringing effects. The spectra were corrected for atmospheric extinction and telluric bands (Bessell 1999; Matheson et al. 2000a), and then flux calibrated using standard stars observed at similar airmass on the same night as the SN (see Table 5). Approximate spectral resolutions were derived from night-sky lines. The wavelength calibration is accurate to about ± 0.2 Å for Kast, from about ± 0.02 Å to ± 0.06 Å (depending on the order) for ESI and about ± 0.08 Å for LRIS. The ISIS spectra were reduced using standard procedures within FIGARO (Shortridge 1991). The wavelength calibration is accurate to about ± 1 Å. The ALFOSC spectrum was reduced using standard procedures within IRAF. The wavelength calibration is accurate to ± 3 Å.

Final fluxing of all except the 397 d spectrum was achieved using near-contemporary VRI photometry taken with the KAIT at Lick Observatory (see Table 2). VRI trans-

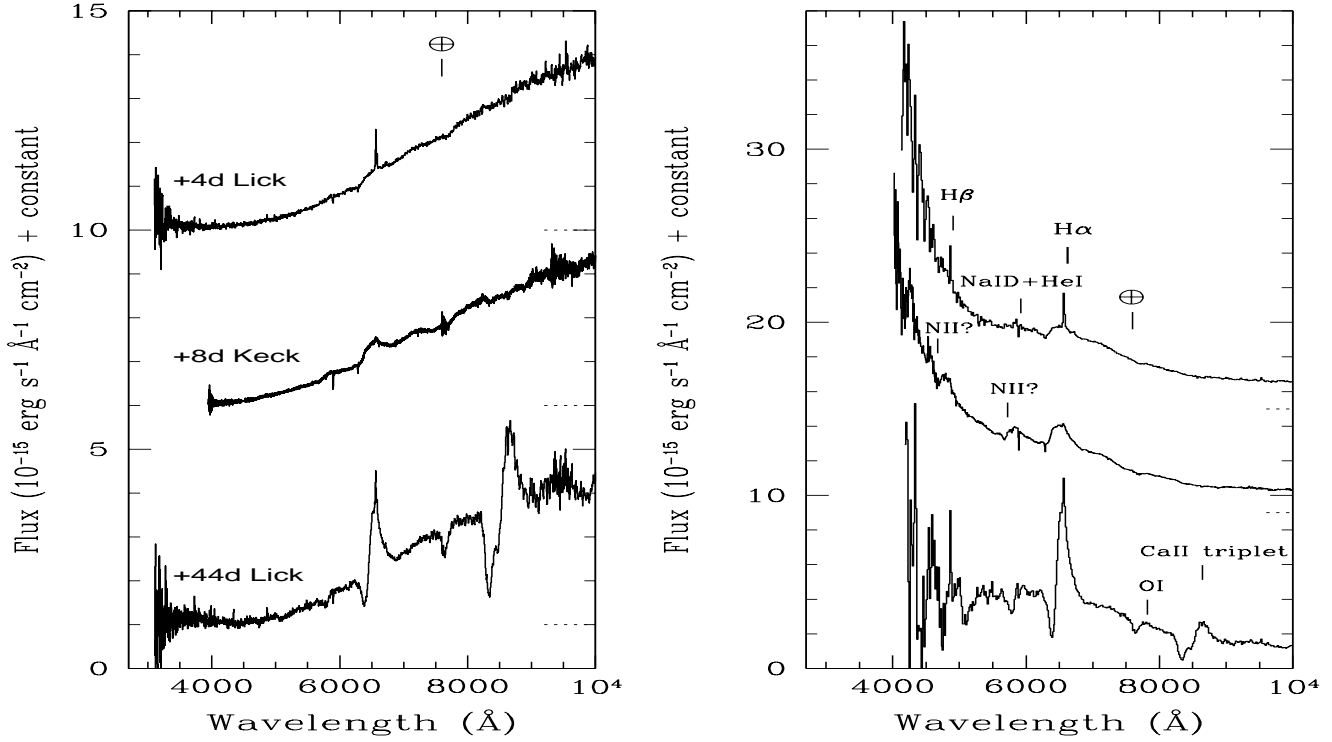


Figure 6. Evolution of the optical spectra of SN 2002hh during the photospheric phase. The left and right panels show the spectra respectively before and after dereddening (see Section 3.2). The spectra have been displaced vertically for clarity (the zero-flux levels are indicated by the dashed lines). No correction has been made for redshift. The narrow emission spikes in the H α (6563 Å) and H β (4861 Å) line profiles are discussed in Section 3. Line identifications are discussed in Section 4. The dereddened spectra have been truncated to remove very low S/N regions towards the blue. Telluric lines are marked.

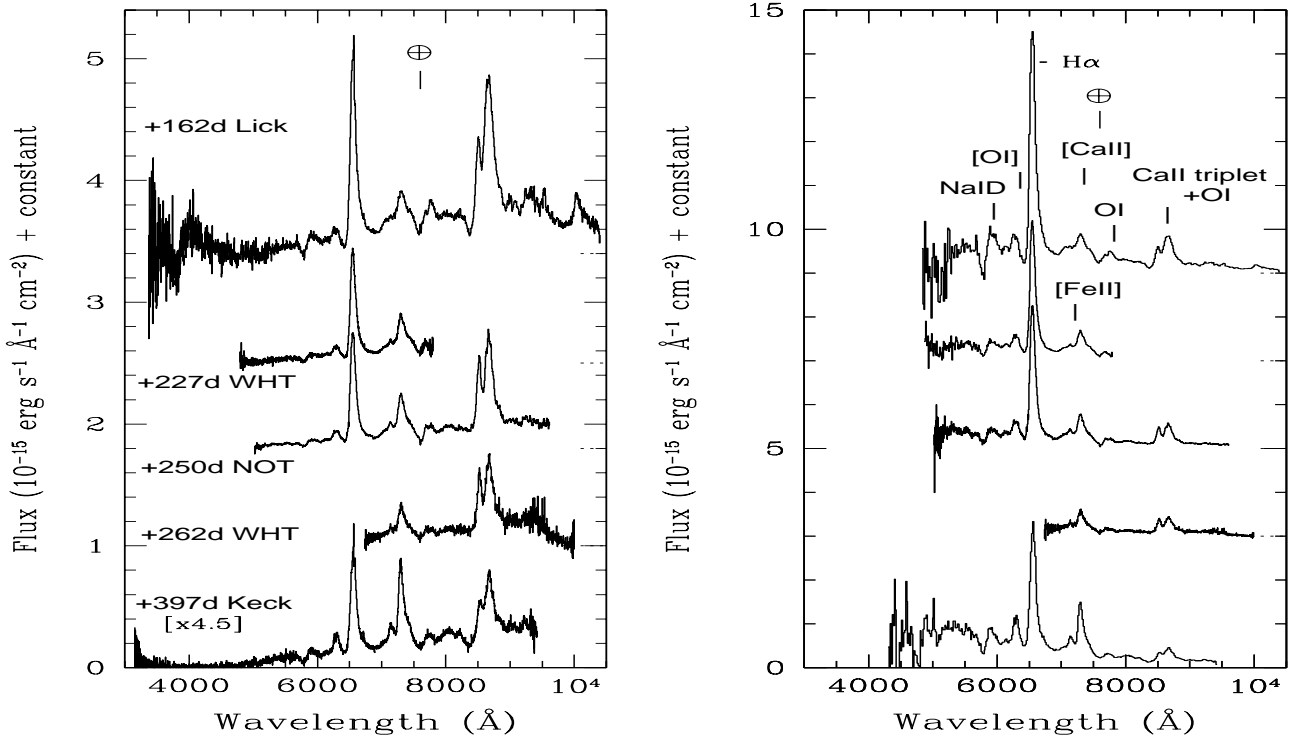


Figure 7. As in Fig. 6, but showing the evolution of the optical spectra of SN 2002hh during the nebular phase.

Table 5. Log of optical spectroscopic observations.

JD ^a	Date	Epoch ^b	Telescope/ Instrument	Range (μm)	Resol.	Slit width/ pos. angle	Spectroscopic standard ^c	Observers
2581.8	2002 Nov 2	4	Lick/Kast ^d	0.31-1.04	600	2''/166°	BD+28°4211, BD+17°4708	A. Filippenko, R. Foley, B. Swift
2585.9	2002 Nov 6	8	Keck/ESI	0.39-1.04	4000	1''/164°	BD+28°4211	A. Filippenko, S. Jha, R. Chornock
2621.8	2002 Dec 12	44	Lick/Kast	0.31-1.04	550	2''/270°	BD+28°4211, HD 19445	R. Foley, M. Papenkova
2738.8	2003 Apr 8	162	Lick/Kast	0.32-1.04	500	2''/79°	Feige 34, HD 84937	R. Foley, M. Papenkova, D. Weisz
2804.7	2003 Jun 14	227	WHT/ISIS	0.47-0.78	1800	1''/176°	BD+17°4798	C. Benn
2828.4	2003 Jul 7	250 ^e	NOT/ALFOSC	0.50-0.96	900	1''/181°	BD+28°4211	J. Sollerman et al.
2839.7	2003 Jul 19	262	WHT/ISIS	0.64-1.03	2050	1''/139°	HD 340611	I. Soechting
2973.9	2003 Nov 29	397	Keck/LRIS ^f	0.31-0.94	1050	1''/127°	BD+28°4211, BD+17°4708	A. Filippenko

^a JD (245 0000+).^b Days after explosion.^c For Kast and LRIS observations, we give the standard stars used respectively for the blue and red part of the combined spectrum.^d Lick observations used a D550 dichroic.^e High temperature and lots of dust reported, very high sky brightness.^f LRIS observations used a D560 dichroic.**Table 6.** Log of IR spectroscopic observations.

JD ^a	Date	Epoch ^b	Telescope/ Instrument	Range (μm)	Resol.	Slit width (arcsec)	Spectroscopic standard	Observers
2714.5	2003 Mar 15	137	IRTF/SpeX	0.81-2.42	1200	0.5	HD 199217	R.D. Joseph, J.T. Rayner
2777.5	2003 May 17	200	IRTF/SpeX	0.80-2.42	2000	0.3	HD 205314	J.T. Rayner
				2.84-4.20	1500	0.5	"	
2843.5	2003 Jul 22	266	IRTF/SpeX	0.80-2.42	2000	0.3	HD 194354	R.D. Joseph, J.T. Rayner
				2.86-4.14	1500	0.5	"	
2891.5	2003 Sep 8	314	IRTF/SpeX	0.80-2.42	2000	0.3	HD 194354	J.T. Rayner
2958.5	2003 Nov 14	381 ^c	IRTF/SpeX	0.93-2.42	750	0.8	HD 194354	R.D. Joseph, J.T. Rayner

^a JD (245 0000+).^b Days after explosion.^c Bad seeing: thick cirrus most of the night, A_K extinction ranging from ~ 1 mag (when spectrum taken) to opaque.

mission functions were formed taking into account the atmospheric transmission function for Lick Observatory, the KAIT imaging filters and the CCD quantum efficiency. These were then applied to the SN 2002hh spectra and to a model spectrum of Vega. The resulting optical spectra were integrated and the total fluxes compared with those of Vega for each *VRI* band to derive spectra-based *VRI* magnitudes. These were then compared with contemporary *VRI* photometric magnitudes derived by interpolation of the light curves. Correction factors ranged from about $\times 0.6$ to $\times 2$. However, there was a tendency for the correction factors to approach closer to unity as we went to longer wavelength bands. This was in spite of efforts having been in most cases made to observe at the parallactic angle. It was found that the variation with wavelength could be reasonably described with linear functions. Linear fits were therefore made to the set of *VRI* correction factors for each epoch. For each wavelength point the effective wavelength was first determined from $\int \lambda F_\lambda d\lambda / \int F_\lambda d\lambda$. The resulting linear function was then used to scale and tilt the corresponding supernova spectrum. The blue limit of the ALFOSC spectrum (250 d) is 5020 Å and consequently does not encompass the full width of the *V*-band transmission function. Therefore only the *R*

and *I* transmission functions were used to derive the flux correction function for this epoch. The wavelength coverage of the ISIS spectra is such that on days +227 and +262 only the *V* band and *I* band respectively are fully spanned by the spectra. Therefore, in these cases only single correction factors were applied viz. $\times 0.97$ for the +227 d spectrum, and $\times 0.7$ for the +262 d spectrum. We judge the accuracy of the final fluxing of the flux-corrected optical spectra to be $\sim \pm 10$ per cent. For the 397 d spectrum, no contemporary photometry was available and so no flux correction was attempted. The fluxing error in this case could be as much as 30 per cent. The optical spectra are shown in Figs. 6 (photospheric phase) and 7 (nebular phase). Each figure comprises 2 panels. The left and right panels show the spectra respectively before and after dereddening. The dereddening is discussed in subsection 3.2. Optical line identification is discussed in Section 4.

2.4 IR spectroscopy

IR spectra were obtained using the 3.0m NASA Infrared Telescope Facility (IRTF) on Mauna Kea (Hawaii), equipped

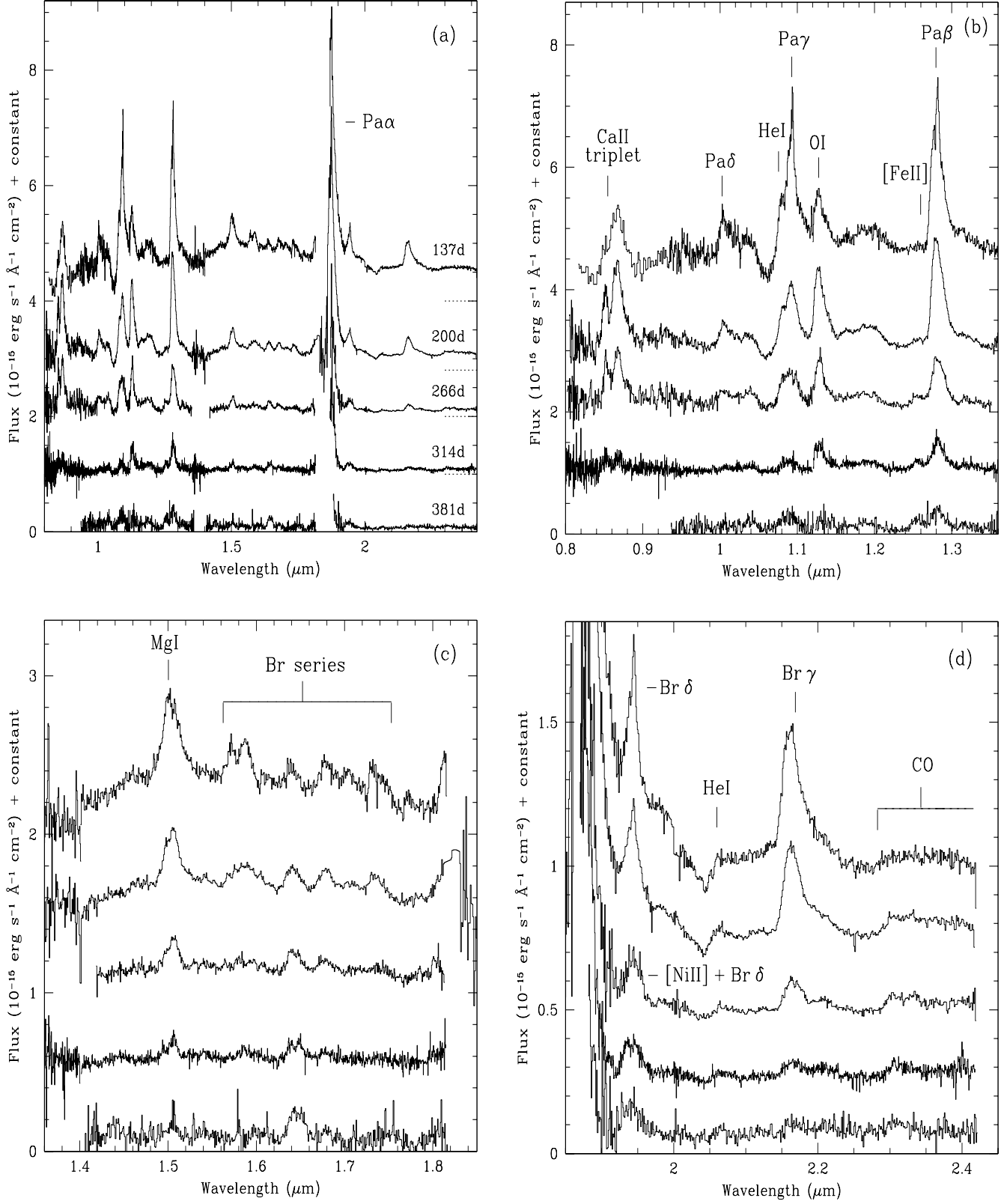


Figure 8. Panel (a): Evolution of the *IJHK*-band IR spectra of SN 2002hh taken at IRTF during the period 137 to 381 days post-explosion. The spectra have been displaced vertically for clarity (the zero-flux levels are indicated by the dotted lines). No correction has been applied for redshift or reddening. Panels (b-d): Detailed subsections of Panel (a) showing, respectively, spectral ranges 0.8-1.36 μm , 1.36-1.85 μm and 1.85-2.45 μm . The detailed evolution of the Pa α 1.875 μm line is shown separately in Fig. 9.

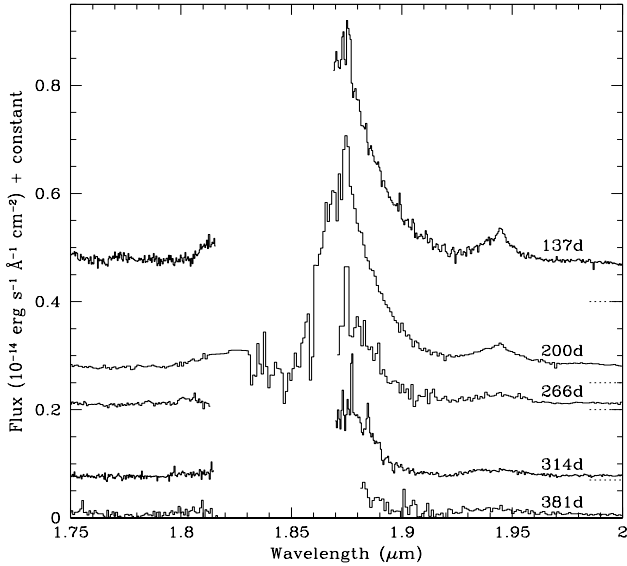


Figure 9. Evolution of the Pa α line from the IR spectra shown in Fig. 8. The spectra have been displaced vertically for clarity (the zero-flux levels are indicated by the dotted lines). The spectra have not been corrected for redshift or reddening.

with SpeX, a medium-resolution 0.8-5.5 μm cryogenic spectrograph and imager (Rayner et al. 2003). We used both the 0.8-2.4 μm cross-dispersed (SXD) and the 1.9-4.1 μm cross-dispersed (LXD) grating modes which provide resolving powers of up to $R \sim 2500$. The spectrograph contains an Aladdin 3 1024 \times 1024 InSb array, with a 0.15 arcsec/pixel scale. *JHK* band spectra were acquired at five epochs, spanning 137–381 days post-explosion. In addition, *I* band spectra were obtained at 4 epochs (137–314 d), and *L'* band spectra were obtained at 200 d and 266 d. See Table 6 for the log of IR spectroscopic observations.

The spectra were reduced using FIGARO (Shortridge 1991). Most of the sky emission was removed by subtraction of successive pairs of exposures taken at two nod positions. The pairs were then coadded. The spectral orders were individually straightened, and residual sky emission lines removed. The spectra were optimally extracted (Horne 1986) and the effects of cosmic rays and bad pixels removed. Wavelength calibration was by means of Argon arc spectra and is accurate to better than $\pm 0.0010 \mu\text{m}$. The telluric standards are listed in Table 6.

Final fluxing of the spectra was by means of the contemporary IR photometry (see Table 4). Transmission functions were formed to represent the combined transmission of the Mauna Kea atmosphere and the SpeX imaging filters. A model atmosphere (IRTRANS) for a water vapour column of 1.6mm and an airmass of 1.5 was used to provide the atmospheric transmission. The filters are the Mauna Kea filter set. Each filter function was multiplied by the atmospheric transmission function to provide net transmission functions in each band. These were then applied to the SN 2002hh spectra and to a model spectrum of Vega. The resulting spectra were integrated and the total fluxes compared with those of Vega for each band to derive spectra-based magnitudes. These were then compared with contemporary pho-

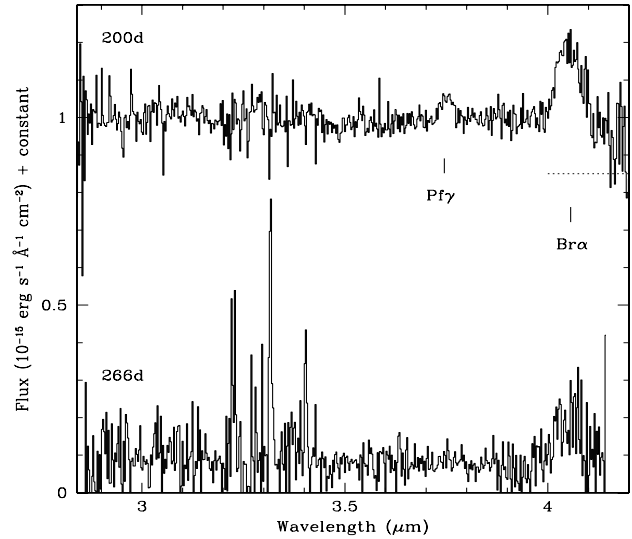


Figure 10. *L*-band IR spectra of SN 2002hh taken, respectively, at 200 d and 266 d post-explosion. The 200 d spectrum has been displaced vertically for clarity (the zero-flux level is indicated by the dotted line). No correction has been applied for redshift or reddening.

tometric magnitudes. For the SXD spectra the dispersion over all epochs in the differences between the spectroscopic and photometric values was about 0.3 magnitudes. This is a respectable value, given the narrowness of the slit and the differences in conditions between the measurements of the supernova and standards. It was also found that at any given epoch a systematic difference existed between the spectroscopic and photometrically-derived magnitudes. We therefore applied corrections to the SXD spectra to bring them more into line with the contemporary photometry. The corrections applied were: day 137- $\times 1.43$; day 200- $\times 0.8$; day 266- $\times 1.03$; day 314- $\times 1.11$. In the *L* band the required corrections were: day 200- $\times 0.51$; day 266- $\times 0.71$. We judge the accuracy of the final fluxing to be $\sim \pm 10$ per cent for the *IJK* band spectra and $\sim \pm 20$ per cent for the *L'* band spectra. For the 381 d spectrum, no contemporary photometry was available and so no flux correction was attempted. The fluxing error in this case could be as much as 50 per cent. The *IJK* band spectra are shown in Fig. 8, while the detailed evolution of the Pa α 1.875 μm line is shown separately in Fig. 9. The *L'* band spectra for epochs 200 d and 266 d are shown in Fig. 10. IR line identification is discussed in Section 4.

The NIR spectroscopic coverage is among the most complete ever achieved for a supernova at late times. Indeed, SN 2002hh is the first ever supernova beyond the Local Group for which *L*-band spectra have been acquired. The temporal coverage of the Pa α line (Fig. 9) is also unsurpassed for a supernova at late-times. The strong atmospheric absorption in this region means that this line has seldom been observed in Type II SNe.

3 REDSHIFT AND EXTINCTION

3.1 Redshift

Strong, narrow Na I D 5890, 5896 Å and K I 7699 Å absorption was detected in the early time spectra. In Fig. 11 we show this spectral region at high resolution on day 8 obtained with Keck/ESI. This reveals two sets of Na I D lines corresponding to velocities of $-20 \pm 10 \text{ km s}^{-1}$ and $+110 \pm 10 \text{ km s}^{-1}$. The K I line has components at $-15 \pm 15 \text{ km s}^{-1}$ and $+113 \pm 10 \text{ km s}^{-1}$. The galactic co-ordinates of SN 2002hh are $l = 95.68^\circ$ and $b = +11.67^\circ$. We suggest that the blue-shifted component is due to absorption within the Milky Way, perhaps within the Perseus Arm. It is unlikely that the $+110/113 \text{ km s}^{-1}$ absorptions are local, given the kinematic distribution of the Milky Way (Martos et al. 2004) and the galactic longitude of SN 2002hh.

Narrow emission lines of H α , H β (4861 Å), [N II] ($\lambda\lambda$ 6548, 6584 Å) and possibly [S II] ($\lambda\lambda$ 6717, 6731 Å) are present, peaking at a redshift of about $+110 \pm 10 \text{ km s}^{-1}$. The narrow lines in the 6300–6800 Å region from 4–397 d are shown in detail in Fig. 14 in the next Section. During the earlier phase, narrow lines are present at 4 d and 44 d at comparable intensity, fade by 162 d and have vanished by 227 d. However, the lines are also completely absent at 8 d. A somewhat broader slit was used on the days when the narrow lines were apparent (see Table 5) and so we suspect that the cause is incomplete background subtraction. HII regions 420 and 421 (Bonnarel, Boulesteix & Marcelin 1986) lie within $3''0$ of the supernova, and may be responsible for the narrow emission. By 397 d, narrow lines have re-appeared. They are unresolved at a resolution of 285 km s^{-1} and are again centred at about $+110 \pm 10 \text{ km s}^{-1}$. They are more than a factor of 10 weaker than at 44 d. Inspection of the 2D frames again suggests that the origin of the narrow lines is due to incomplete background subtraction. While a relatively narrow $1''0$ slit was used at 397 d, the much weaker ejecta emission by this epoch is probably the reason that residual narrow lines from the background have become apparent. That the narrow emission lines show redshift velocities consistent with the $\sim +110 \text{ km s}^{-1}$ derived from the Na I D and K I absorptions, may indicate a physical association between the H II regions and the line-of-sight absorbing material.

We adopt $+110 \pm 10 \text{ km s}^{-1}$ as the redshift of the SN centre-of-mass, although neither the narrow absorption lines nor narrow emission lines necessarily have any physical connection with the supernova. This value is much larger than the redshift of the host galaxy ($+48 \pm 10 \text{ km s}^{-1}$): the difference is probably caused by the rotation of NGC 6946.

3.2 Extinction

As mentioned in the Introduction, the extinction to SN 2002hh is very high. To estimate and correct for the extinction, we compared the spectra and light curves of SN 2002hh with those of SN 1999em. The justification for this was that the light curves of both supernovae indicate that both events were normal Type IIP. We therefore assumed that the two events were identical, and endeavoured

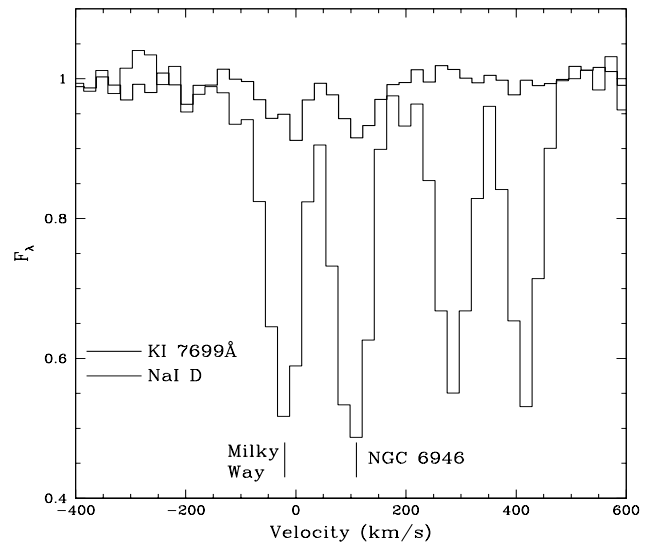


Figure 11. Interstellar absorption lines towards SN 2002hh at +8 days. The thick (upper) line is K I 7699 Å and the thin (lower) line is the Na I D doublet. The spectra are plotted in velocity space relative to the rest frames of the K I and Na I D1 lines respectively. The Na I D2 line can also be seen at the RHS. Each line has two components produced by absorption in, respectively, the Milky Way and NGC 6946. The lines are unresolved at a resolution of 75 km s^{-1} .

to match their coeval optical spectra (epoch $\sim +7$ days) by adjusting the amount of dereddening for SN 2002hh. We adopted the Cardelli et al. (1989) extinction law, initially with $R_V = 3.1$. For the SN 1999em extinction we took $A_V = 0.31 \text{ mag}$ (Baron et al. 2000) and for the explosion epoch we adopted JD2451475.4 (=1999 Oct. 23.9), which is the weighted mean of the estimates of Baron et al. (2000), Hamuy et al. (2001), Leonard et al. (2002a) and Elmhamdi et al. (2003). The SN 1999em spectrum was also scaled by $\times 4$ to allow for the difference in distance (cf. Leonard et al. 2003). However, we found that no value of A_V would provide a satisfactory match between the spectra. We therefore allowed both A_V and R_V to vary. From this, we found that satisfactory matches could be obtained with $A_V(\text{SN 2002hh}) = 5.2 \pm 0.2 \text{ mag}$ and $R_V = 1.9 \pm 0.2$.

As a check on the above extinction estimate, we examined the narrow Na I D and K I interstellar absorption lines (Fig. 11). At such a high extinction (see above), it is recognised (e.g. Munari & Zwitter 1997) that the equivalent width (EW) of Na I D is of little value since the lines are too close to saturation. That this is the case here is confirmed by the EW ratio of the Na I 5890 Å to 5896 Å lines which is 1.2 for the Milky way and 1.3 for NGC 6946 (towards SN 2002hh) i.e. both are close to the total saturation ratio of 1.1 and far from the unsaturated value of 2.0. However, the K I line is expected to remain unsaturated for much higher extinctions (Munari & Zwitter 1997). We obtain K I line EW values of $0.131 \pm 0.021 \text{ Å}$ and $0.146 \pm 0.026 \text{ Å}$ for the Milky Way and NGC 6946 respectively. From the EW v. E(B-V) curve of Munari & Zwitter (1997) we deduce corresponding E(B-V) values of 0.50 and 0.57 mag. The former is reasonably consistent with the E(B-V)=0.34 mag value from the far-IR maps of Schlegel et al. (1998). For $R_V \sim 3$, the latter

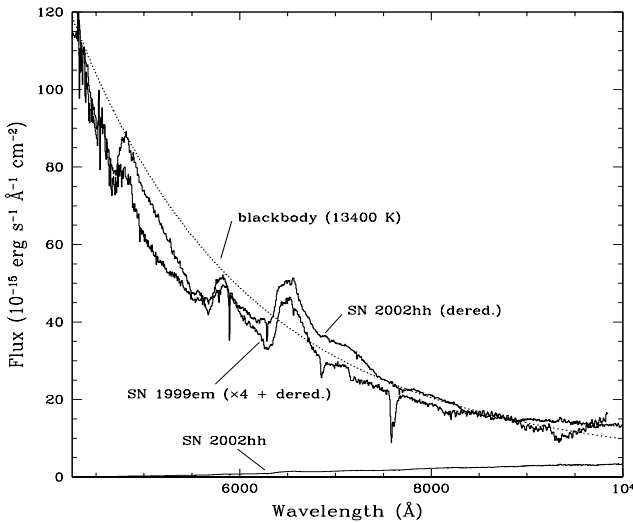


Figure 12. Comparison of coeval spectra of SN 2002hh and SN 1999em taken at about +7 days post-explosion. The SN 2002hh spectrum has been dereddened according to the 2-component extinction model *viz.* $A_V = 3.3$ mag, $R_V = 3.1$ plus $A_V = 1.9$ mag, $R_V = 1.1$ (see text for details). The SN 1999em spectrum has been dereddened with $A_V = 0.31$ mag, $R_V = 3.1$, and scaled by $\times 4$ to correct for the difference in distance between the two SNe. The extinction law of Cardelli et al. (1989) was used in both cases. Also shown is a blackbody curve for a temperature of 13,400 K. The faint red spectrum near the bottom is the original un-dereddened spectrum of SN 2002hh plotted on the same scale. This illustrates the very large extinction correction that has been applied. In spite of this, the dereddened spectra of the two SNe appear remarkably similar.

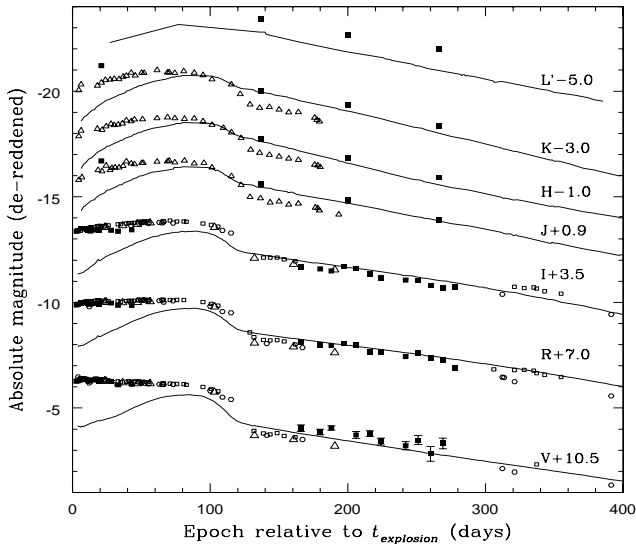


Figure 13. De-reddened absolute magnitude optical and NIR light curves of SN 2002hh (filled squares) compared with those of the Type IIpec SN 1987A (lines) and the Type IIP SN 1999em (open squares - Leonard et al. 2002a; triangles - Hamuy et al. 2001, see text for details; circles - Elmhamdi et al. 2003). For clarity, the light curves have been displaced vertically by the amounts indicated at the RHS. See text for further details. Note that the early SN 2002hh IR points are J and K at +21 d (see also text).

is consistent with the $A_V = 1.2^{+1.3}_{-1.7}$ mag which Barlow et al. (2005) derive from the extinction profiles of Holwerda et al. (2005). However, Munari & Zwitter caution that the derived $E(B-V)$ may be an overestimate if the absorption line is formed by unresolved multi-component emission. Alternatively, the presence of a dense “dust pocket” might not be traced by the absorption lines, leading to an underestimate of $E(B-V)$. Notwithstanding these comments, the total $E(B-V) = 1.07$ mag corresponding to only $A_V = 3.3 \pm 0.3$ mag ($R_V = 3.1$). Taken at face value, this suggests that the remaining $A_V = 1.9 \pm 0.2$ mag of the total 5.2 mag extinction was unrevealed by the K I lines. This additional extinction may be associated with the line-of-sight H II regions and so did not show the correlation with the K I absorption EW which occurs in H I regions. To investigate this further, we dereddened the day +8 SN 2002hh spectrum using a 2-component extinction where the first component, due to the combined effect of the ISMs of the Milky Way and NGC 6946, was assigned $A_V = 3.3$ mag and $R_V = 3.1$. A second component was then added, with A_V and R_V as free parameters. A satisfactory match was obtained with $A_V = 1.9$ mag and $R_V = 1.1$ for the second component. The dereddened spectra of SNe 1999em and 2002hh are shown in Fig. 12. Also shown is the spectrum of a blackbody corresponding to $T = 13,400$ K and an expansion velocity of $6,800$ km s $^{-1}$, with the expansion beginning 7 days previously. While the value obtained for R_V is small, such values have been invoked in the past in multi-component extinction models (see Wang et al. 2004 and refs. therein). It implies that the “dust pocket” grain size is small compared with the average value for the local ISM. Also, as already indicated, the EW-derived ISM extinction may be an overestimate. A smaller ISM extinction would allow a larger “dust pocket” extinction and hence a larger value for R_V , with the upper limit being the $R_V = 1.9$ mag obtained in the single component case.

As noted in the Introduction, Pooley & Lewin (2002) derived a column density of $N_H = 10^{22}$ cm $^{-2}$ from their X-ray data. Adopting $A_V = 0.53 \times 10^{-21} [N(\text{HI}) + 2N(\text{H}_2)]$ (Bohlin, Savage & Drake 1978) we obtain $A_V = 5.3$ mag in good agreement with the values derived from spectral matching and the K I IS lines.

In Fig. 13 we show the dereddened absolute magnitude optical and IR light curves of SN 2002hh and SN 1999em, as well as those of the peculiar Type II SN 1987A. To the data for SN 2002hh we have added the +21 d J and K points of Meikle et al. (2002), which correspond to dereddened absolute magnitudes of $M(J) = -17.6$ and $M(K) = -18.2$. The SN 1999em optical magnitudes are from Hamuy et al. (2001), Leonard et al. (2002a) and Elmhamdi et al. (2003). The IR magnitudes of SN 1999em are instead from Fig. 1 of Hamuy et al. (2001): no tabulated data were presented there nor these were subsequently published as stated in the paper. The optical magnitudes for SN 1987A are from Hamuy et al. (1988) and Suntzeff et al. (1988), *JHK* magnitudes from Bouchet et al. (1989) and Bouchet & Danziger (1993), and *L'* magnitudes from Catchpole et al. (1988) and Whitelock et al. (1988). Dereddening of the SN 1999em and SN 2002hh light curves was by means of, respectively, the single component and 2-component extinction laws de-

scribed above. The adopted distances are: SN 2002hh - 5.9 Mpc (see above); SN 1999em - 11.7 Mpc (Leonard et al. 2003). For SN 1987A we used a distance of 51.4 kpc and an $A_V = 0.6$ mag (Romaniello et al. 2000, 2002). Its magnitudes were dereddened using the Cardelli et al. law with $R_V = 3.1$.

Since the A_V and R_V values used for dereddening the SNe 1999em and 2002hh light curves were obtained by matching their day +7 optical spectra, we checked that a match was also obtained between the *VRI* light curves of the two supernovae at around +7 d. In the *R* and *I* bands a good match (difference < 0.1 mag) was indeed found. However, in the *V*-band, the SN 2002hh magnitude was about 0.3 mags fainter than that of SN 1999em, in spite of the good match obtained between the spectra in this wavelength range. We attribute this discrepancy to differences in the true effective wavelengths (used in the light curve dereddening) of the *V*-band between the two SNe due to the large difference in extinction together with the intrinsically steep spectral slope. We find that by shifting the effective wavelength of the *V*-band for SN 2002hh to the blue by 200 Å a good match is obtained at +8 d. The same effective *VRI* wavelengths are used for dereddening the optical light curves at all epochs. This may explain, at least partly, why the light curve match between SNe 1999em and 2002hh becomes poorer at later epochs.

The optical light curves of SNe 1999em and 2002hh are generally well-matched in both the photospheric and nebular phases. The early-time difference with respect to SN 1987A is not surprising given its rather different nature. Nevertheless, the radioactive tails of all three supernovae match reasonably well in the optical. In the NIR, the early-time difference between SN 1987A and SN 2002hh is similar to that seen in the optical. However, in contrast to the optical region, by 266 d the *HK* luminosities of SN 2002hh slightly exceed those of SN 1987A. Moreover the excesses increased by 314 d. In addition the L' luminosity of SN 2002hh is significantly brighter than that of SN 1987A from as early as 137 d, and this excess also shows some sign of increasing with time. This “IR excess” is discussed below. The NIR light curves of SNe 1999em and 2002hh, while consistent with having similar shapes, display what appears to be an approximately constant relative offset of 0.5–0.7 magnitudes spanning 10 to 200 days, with SN 1999em being the fainter of the two. Given the good optical match between SNe 1999em and 2002hh at early times, and between all 3 supernovae during the radioactive tail, this large NIR mismatch between SN 1999em and 2002hh is puzzling. The occurrence of this mismatch both at early times and in the J-band rules probably out emission from warm dust in SN 2002hh (see below) as the source of this difference. We have tried to match the light-curves by leaving both R_V and A_V as free parameters, but no satisfactory match was found for the *VRIJHK* photometry, not even with the two dust component model: while the optical light-curves agree, the IR light-curves are always offset by the amount specified above. We therefore suspect that a spurious systematic offset is present in the SN 1999em NIR data, possibly related to the IR calibrations.

The above analysis confirms that the extinction towards

SN 2002hh is high and that the bulk of it occurs within NGC 6946. There is some indication that the extinction within NGC 6946 comprises two components. One of these has an exceptionally small R_V and is not traced by the K I absorption lines. It may be due to a localised dust cloud associated with line-of-sight H II regions.

3.3 OIR luminosity and the ^{56}Ni mass

As explained above, we derived the total extinction by assuming that SN 1999em and SN 2002hh were alike in the optical region at about 1 week-post explosion. The fact that the subsequently de-reddened *VRI* absolute light curves also agree to as late as ~ 270 days tends to support the validity of this assumption. We also find good agreement with the late-time *VRI* tails of SN 1987A. From these matches we conclude that the mass of ^{56}Ni ejected by SN 2002hh was similar, *viz.* $(0.08 \pm 0.01) M_\odot$.

A more direct approach to estimating the mass of ^{56}Ni ejected is by determining the total late-time luminosity during the radioactive tail. During the earlier part of the nebular phase, Type II SNe become largely optically thin to UVOIR radiation, but remain optically thick to the high energy gamma rays from the radioactive decay. Thus, in principle, the late-time UVOIR light curve can allow us to estimate the amount of ^{56}Ni produced in the SN explosion. The problem in attempting such an analysis for SN 2002hh is the enormous extinction correction required. One possible concern is that we have no useful data shortward of the *V* band which cuts off at about 4300 Å. However, given the late epochs considered, this may only result in a small underestimate. In SN 1987A at 203 d the luminosity peaked in the *I*-band while less than 2 per cent of the total was emitted shortward of 4300 Å (Catchpole et al. 1988, Fig. 4). Thus, if the similarity of SN 2002hh to SN 1987A is maintained at these shorter wavelengths, we can safely ignore the lack of *UB* band data. Nevertheless, even in the *I*-band we estimate an extinction reducing the flux by a factor of $\times(8 \pm 1)$.

We have estimated the ^{56}Ni mass in SN 2002hh using our late-time *VRIJHKL'* photometric data obtained at 200 d and 266 d to derive “*OIR*” luminosities. The optical and IR magnitudes (see Tables 2 and 4) were converted into fluxes at the effective wavelengths of the filters using the flux calibrations of Bessell (1979) and those of Bersanelli, Bouchet & Falomo (1991) respectively. Adopting the two-component extinction model ($A_{V1} = 3.3 \pm 0.3$ mag, $R_{V1} = 3.1$; $A_{V2} = 1.9 \pm 0.2$ mag, $R_{V2} = 1.1$) (see above), the fluxes were then de-reddened according to the Cardelli et al. (1989) extinction law. The total fluxes at the two epochs were then derived by fitting spline curves (Press et al. 1992) to the de-reddened *VRIJHKL'* fluxes and integrating over the wavelength range λ 4288–44993 Å using a trapezoidal rule (the range is fixed by the limits of the filter functions used in the photometric observations) (see Table 7, col. 2). Finally, the *OIR* luminosities were derived from the total fluxes by adopting a distance of 5.9 ± 0.4 Mpc to the host galaxy (see Table 7, col. 3). The reported errors take into account the internal errors from the spline fit plus the uncertainties in both the distance and extinction values. As

Table 7. OIR flux and luminosity of 02hh in the nebular phase.

Epoch (days)	F_{OIR}^a (10^{-10} ergs s $^{-1}$ cm $^{-2}$)	L_{OIR}^b (10^{41} ergs s $^{-1}$)
200	0.442(0.053)	1.84(0.25)
266	0.215(0.034)	0.89(0.16)

^a, ^b Error given in brackets; see text.

discussed below, a fraction of the IR luminosity may be due to an IR-echo. At 200 d and 266 d the echo model described below suggests that around 10 per cent of the late-time luminosity could have been due to an echo.

The mass of ^{56}Ni ejected from SN 2002hh is obtained from $M(^{56}\text{Ni}) = M(^{56}\text{Ni})_{87A} \times L_{02hh}/L_{87A} M_{\odot}$, where $M(^{56}\text{Ni})_{87A}$ is the mass of ^{56}Ni produced by SN 1987A, L_{02hh} is the OIR luminosity of SN 2002hh and L_{87A} is the coeval UVOIR luminosity of SN 1987A. We adopt $M(^{56}\text{Ni})_{87A} = 0.073 \pm 0.012 M_{\odot}$, which is the weighted mean of values given by Arnett & Fu (1989) and by Bouchet, Danziger & Lucy (1991), and includes uncertainties in distance and extinction. Thus, for SN 2002hh we obtain an ejected ^{56}Ni mass of $0.08 \pm 0.02 M_{\odot}$ (where the given error includes the uncertainty in the distance and extinction of SN 2002hh plus the uncertainty in the ^{56}Ni mass of SN 1987A). Reducing this by 10 per cent to allow for the IR echo contribution, we obtain $0.07 \pm 0.02 M_{\odot}$. To within the errors, this is the same value as obtained above from the similarity of the VRI light curves. The large uncertainty is primarily due to the large extinction correction.

Similar coeval luminosities for the [Fe II] 1.257 μm line are obtained in SNe 1987A and 2002hh although the SN 2002hh values are of low S/N (see Fig. 21 in Section 5). Assuming a similar ionisation degree and temperature for the two SNe and that most of the iron results from the decay of ^{56}Ni , this provides additional support for our conclusion that similar masses of ^{56}Ni were ejected by the two SNe.

4 SPECTROSCOPIC BEHAVIOUR

4.1 Overview

4.1.1 Photospheric phase

During the photospheric phase, the 4 d and 8 d dereddened optical spectra (Fig. 6, RHS) are characterized by a blue continuum with few discrete features. Broad, low-contrast P Cygni-like H α is visible at 4 d, together with H β 4861 \AA , He I 5876 \AA and strong, narrow (interstellar) Na I D absorption (see section 3.1). Narrow emission lines of H α and H β are also present and are probably due to nearby HII regions (see section 3.1). By 44 d, following the typical spectral evolution of Type IIP SNe, the broad H α and H β P Cygni emission had become much more prominent while the blue continuum had faded significantly. In addition, broad P Cygni lines of O I 7773 \AA and the Ca II triplet had appeared.

In the 8 d spectrum, features occur at about 4600 \AA and

5500 \AA . Similar features are also visible in near-coeval spectra of SN 1987A, SNe 1999em and 1999gi (see Elmhamdi et al. 2003; Leonard et al. 2002b). For SN 1999em, Baron et al. (2000) suggest N II \sim 5679 \AA (multiplet 3) as the origin of the second of these. Recently, Dessart & Hillier (2005) have presented a quantitative spectroscopic analysis of the photospheric phase of Type IIP SNe: from synthetic fits to early-time spectra they confirm the Baron et al. identification. They conclude that the 4600 \AA and 5500 \AA features in SNe 1987A, 1999em and 1999gi are due, respectively, to N II \sim 4623 \AA (multiplet 5) and N II \sim 5679 \AA (multiplet 3). We therefore propose that the 4600 \AA and 5500 \AA features in the 8 d spectrum of SN 2002hh are also due to the N II multiplets. As pointed out by Dessart & Hillier, this indicates an overabundance of nitrogen in the outer layers of the progenitor star prior to core-collapse.

4.1.2 Nebular phase

In our investigation of the nebular phase spectra (Figs. 7–10), we were guided by the spectroscopic studies of SN 1987A performed by Meikle et al. (1989; 1993) and Spyromilio et al. (1991). The optical and NIR spectra are dominated by broad emission lines of neutral or singly-ionised species. In Tables 8 and 9 we list, for the optical and NIR regions respectively, the identifications of the stronger nebular-phase lines (uncorrected for redshift) together with their intensities. The evolution of the velocity widths for the most prominent single emission lines is described in Table 10. In the optical region, a weak flat continuum is present up to at least 262 d (see Fig. 7, RHS). However, by the time the SN is recovered on day 397 d, a strong blue continuum has developed. A strong persistent IR continuum was also present in the nebular phase and this is discussed in the next section.

4.1.3 Individual Elements

Hydrogen and Helium

The late-time spectra (see Figs. 7, 8) are dominated by broad H α emission together with lines of the Paschen and Brackett series. H β is undetected. Given a typical intrinsic H β /H α intensity ratio plus the high extinction, this is unsurprising. Pf γ can be seen in the day 200 2.85–4.15 μm spectrum (see Fig. 10). Strong He I 1.083 μm and 2.058 μm are also present. Both He I features show P Cygni-like troughs which persist right up to the last epoch. As the supernova evolved, the H lines gradually weakened with respect to other lines. The H/He line profiles and their evolution are discussed later.

Oxygen

We identify the strong 1.13 μm feature with the O I 1.129 μm Bowen resonance fluorescence line. Ly β photons pump the 1025 \AA triplet and the subsequent cascade feeds the O I 8446 \AA and 1.129 μm lines. An alternative identification is [S I] 1.131 μm (the other [S I] line at 1.082 μm would be blended with He I). However, the O I 1.129 μm identification is confirmed by the presence of the strong narrow

Table 8. Optical emission features observed on days 162 to 397 in SN 2002hh.

ID	Epoch (days)	λ_{peak} (Å)	Intensity (10^{-13} erg s $^{-1}$ cm $^{-2}$)
[O I] 6300, 6364 Å	162	6267	0.16
	227	6298	0.09
	250	6304	0.08
	262	–	–
	397	6300	0.03
H α 6563 Å ^a	162	6543	1.50
	227	6545	0.86
	250	6546	0.73
	262	–	–
	397	6554	0.18
[Ca II] 7291, 7323 Å	162	7303	1.00
	227	7298	0.43
	250	7303	0.54
	262	7305	0.39
	397	7298	0.17
O I 7771 Å + K I 7676 Å	162	7763	0.82
	227	7678	0.18
	250	7770	–
	262	7685	0.16
	397	7718	0.05
O I 8446 Å + Ca II 8498 Å	162	8505	0.77
	227	–	–
	250	8517	0.63
	262	8520	0.50
	397	8529	0.11
Ca II 8542 Å + Ca II 8662 Å	162	8676	2.44
	227	–	–
	250	8662	1.32
	262	8672	0.99
	397	8677	0.24

^a The H α 6563 Å intensity excludes, when present, interstellar nebular emission (*cf.* 162d and 397 d spectra).

feature at ~ 8500 Å (see Fig. 7) which we identify with the O I 8446 Å line, blended with the Ca II IR triplet. The O I 1.129 μ m line increased in prominence during the 137–314 d period with respect to Pa γ (see Table 9 for details). In addition, its width narrowed up to day 266. Its presence is important since, for the Bowen mechanism to operate, there must have been intimate mixing of hydrogen and oxygen. Other oxygen lines visible in our spectra include [O I] 6300/64 Å and O I 7771 Å (probably blended with K I 7676 Å), although the different components are not resolved. The P-Cygni absorption may be affected by the uncorrected telluric absorption at ~ 7600 Å.

Sodium

By 162 d, the broad He I 5876 Å P Cygni line had given way to a P Cygni feature due to Na I D. The presence of sodium emission is confirmed by Na I 2.206 μ m emission, initially seen as a red wing to the Br γ line. In addition, the red wing of the O I 1.13 μ m feature is probably due to the Na I 1.138 μ m doublet.

Magnesium

We identify the strong 1.5 μ m feature with Mg I 1.503 μ m. This dominated the *H*-window to day 266 but faded quite rapidly thereafter. Its optical transition at 8807 Å probably contributes to the red wing of the Ca II triplet.

Silicon

At all five epochs a broad feature in the 1.16–1.22 μ m range is present. The same feature occurred in SN 1987A and was attributed to a blend of K I(multiplet 6), Mg I(6) and Si I(4) by Meikle et al. (1989). However, Fassia, Meikle & Spyromilio (2002) noted that, given this multiple origin, the constancy of the shape between days 112 and 1822 is remarkable and may argue against a blend of different species. The virtual absence of [Si I] 1.6068 μ m emission in SN 2002hh suggests a significantly lower silicon abundance than was seen in SN 1987A (see section 5.2).

Calcium

The Ca II IR triplet is prominent in both the optical and

Table 9. IR emission features observed on days 137 to 381 in SN 2002hh.

ID	Epoch (days)	λ_{peak} (μm)	Intensity (10^{-13} erg s $^{-1}$ cm $^{-2}$)
Ca II triplet 0.85-0.87 μm	137	0.871	1.49
	200	0.867	3.74
	266	0.867	2.21
	314	–	–
	381	–	–
Pa δ 1.005 μm + ? ^(a)	137	1.003	0.92
	200	1.003	1.20
	266	–	–
	314	–	–
	381	–	–
Pa γ 1.094 μm + He I 1.083 μm	137	1.093	2.57
	200	1.092	2.29
	266	1.090	1.51
	314	1.095	0.51
	381	1.094	0.52
O I 1.129 μm	137	1.128	1.23
	200	1.127	1.67
	266	1.130	0.88
	314	1.128	0.66
	381	–	–
Pa β 1.282 μm	137	1.281	3.60
	200	1.279	2.66
	266	1.279	1.40
	314	1.281	0.73
	381	1.281	0.62
Mg I 1.503 μm	137	1.501	0.87
	200	1.505	0.68
	266	1.507	0.36
	314	1.506	0.16
	381	1.505	0.08
Pa α 1.875 μm	137	1.876	–
	200	1.875	7.75
	266	1.875	3.70
	314	1.878	1.10
	381	–	–
Br δ 1.945 μm	137	1.944	0.81
	200	1.944	0.76
	266	1.938	0.50
	314	1.945	0.34
	381	1.945	0.40
Br γ 2.166 μm	137	2.162	1.08
	200	2.162	0.86
	266	2.162	0.32
	314	2.164	0.20
	381	–	–
Pf γ 3.740 μm	200	3.750	0.29
Br α 4.051 μm	200	4.056	1.37

^a This feature is blended with an unidentified feature around 1.03 μm . The given intensity is for the whole double-peaked feature at peak emission.

IR spectra, probably blended with O I 8446 Å, and possibly with [C I] 8727 Å and Mg I 8807 Å. We also identify the [Ca II] 7291,7323 Å feature. [Fe II] 7388,7452 Å may be possibly contributing to its red wing. The lack of prominent emission at 1.99 μm tends to rule out a significant contribution from Ca I 1.94,1.98 μm.

Iron, Cobalt, Nickel

We identify [Fe II] 1.257 μm and possibly [Fe II] 1.644 μm in the NIR plus a weaker feature in the optical region due to [Fe II] 7155 Å. [Fe II] 1.257 μm became increasingly prominent with time and by 381 d was quite significant despite the low S/N of the spectrum (partly due to atmospheric conditions, see note in Table 6). In the 1.4 – 1.8 μm window, as the Brackett lines faded, a prominent feature at ~1.643 μm emerged, probably due to [Fe II] 1.644 μm. While [Si I] 1.645 μm may also have been contributing there is little sign of the other component of this doublet at 1.607 μm which should be 40 per cent of the 1.645 μm intensity. We conclude that [Si I] 1.645 μm made at most a minor contribution. In Section 3.3 above, we have used the [Fe II] 1.257 μm line to estimate the mass of ejected ⁵⁶Ni.

There is little sign of [Co II] 1.547 μm emission. In SN 1987A during the period 255–377 days the intensity ratio of the features at 1.54 μm (a blend of [Fe II] 1.533 μm and [Co II] 1.547 μm) and 1.64 μm was typically 0.25. Thus, given the relatively low S/N of the 1.64 μm feature in SN 2002hh during this period, it is likely that the 1.54 μm feature is buried in the noise.

As Br γ and Br δ faded it is clear that by 266 d another species was contributing to the feature at 1.94 μm. By the final epoch, this feature is the most prominent in this window. In SN 1987A Meikle et al. (1989, 1993) attributed this to a blend of Br δ, Ca I 1.94 μm and [Ni II] 1.94 μm (plus a small contribution from [Fe II] 1.95 μm). They found that at 377 d the [Ni II] line contributed 30% of the blend, increasing to 60% by 574 d. However, any Ca I 1.94 μm contribution should be accompanied by a comparably strong Ca I 1.98 μm feature. The lack of a strong emission feature at 1.98 μm in SN 2002hh tends to rule out a significant contribution of Ca I to the 1.94 μm blend during the 266–381 d period, although it may have made a more significant contribution at earlier epochs. We conclude that by 266 d the 1.94 μm feature is a blend of [Ni II] 1.94 μm and Br δ.

Carbon Monoxide

CO first overtone emission is detected by 137 d. As time passes the longer wavelength components fade faster as the cooling ejecta depopulates the higher vibrational levels (cf. Spyromilio et al. 1989). The presence of CO emission is important as it may presage the condensation of dust in the ejecta (see Introduction). The CO temporal evolution in the period 137–381 d is discussed in detail in Section 5.2.1.

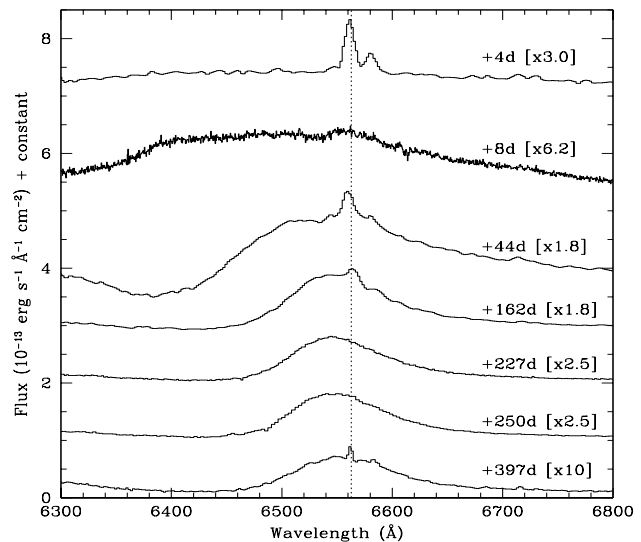


Figure 14. Evolution of the H α emission line profile during the 4–397 d period. The spectra have been de-reddened and redshift-corrected, and have been displaced vertically for clarity. The vertical dotted line corresponds to the adopted redshift of 110 km s⁻¹ for the SN centre of mass (see text). Narrow emission lines of H α , [N II] ($\lambda\lambda$ 6548, 6584 Å) and [S II] ($\lambda\lambda$ 6717, 6731 Å) from the HII regions are also visible (see Section 3 for details).

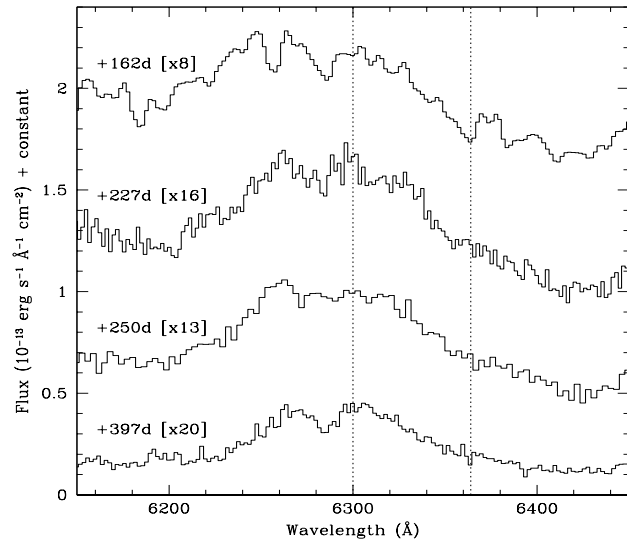


Figure 15. As in Fig. 14, but showing the evolution of the O I 6300,6363 Å emission line profile during the nebular phase.

4.1.4 Nebular line-profile evolution

In Figs. 14 to 19 we show the evolution of the most prominent, isolated lines. In all these plots, the rest-frame wavelengths of the lines are indicated by vertical dotted lines. As the supernova evolved, the H lines gradually weakened with respect to other lines. Due to difficulty in disentangling contribution from other species, we were able to measure the velocity widths (FWHM) and shifts of just H α in the optical region, and of O I, Pa β , Mg I and Br γ in the IR region. The line widths and shifts are listed in Table 10.

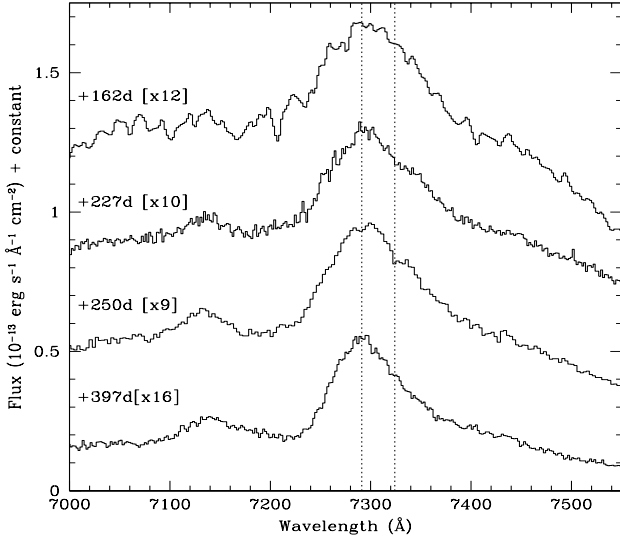


Figure 16. As in Fig. 14, but showing the evolution of the [Ca II] 7291,7323 Å emission line profile during the nebular phase.

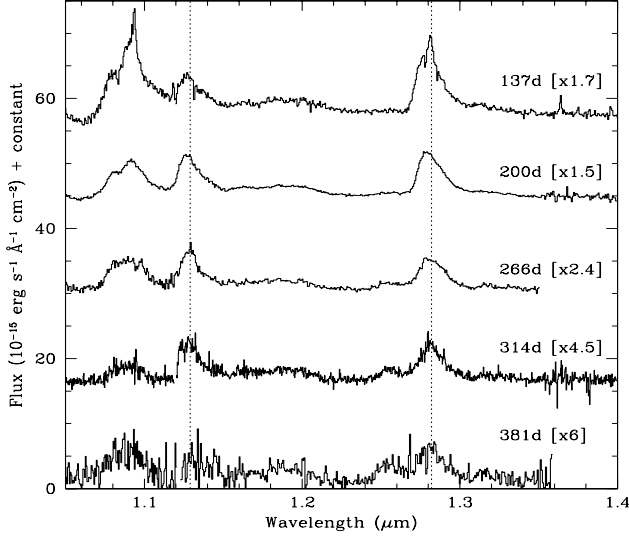


Figure 17. Evolution of the O I (1.129 μm) and of the Paβ (1.282 μm) emission lines in SN 2002hh (days 137 to 381). All the spectra have been de-reddened and shifted to the rest frame.

During the nebular phase, linewidths of around 3800–4600 km s⁻¹ (FWHM) are seen in the hydrogen lines. There is weak evidence of a modest decline in the widths of the other lines with time. During the earlier part of the nebular phase both the Balmer and Paschen lines tend to be asymmetric with enhanced red wings. The profiles of [O I] 6300,64 Å and Mg I 1.503 μm (see Figs. 15, 18) exhibit pronounced irregularities during the earlier part of the nebular phase. This may indicate clumping in the SN ejecta as was inferred for SNe 1987A and 1993J (Matheson et al. 2000b and refs. therein). In contrast, the lack of well defined small-scale structures in [Ca II] 7291,7323 Å (see Fig. 16) suggests that calcium is more uniformly distributed in the SN ejecta. The [Ca II] feature does exhibit a persistent asymmetry with an extended red wing. However, a 3/2 intensity

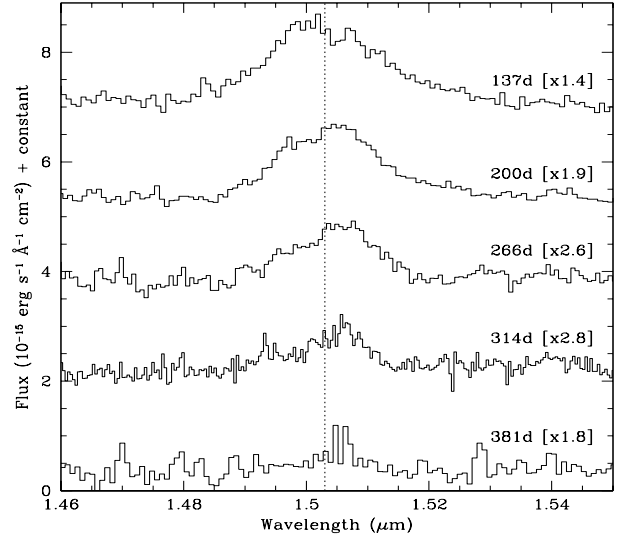


Figure 18. As in Fig. 17 but showing the evolution of the Mg I 1.503 μm emission line in SN 2002hh.

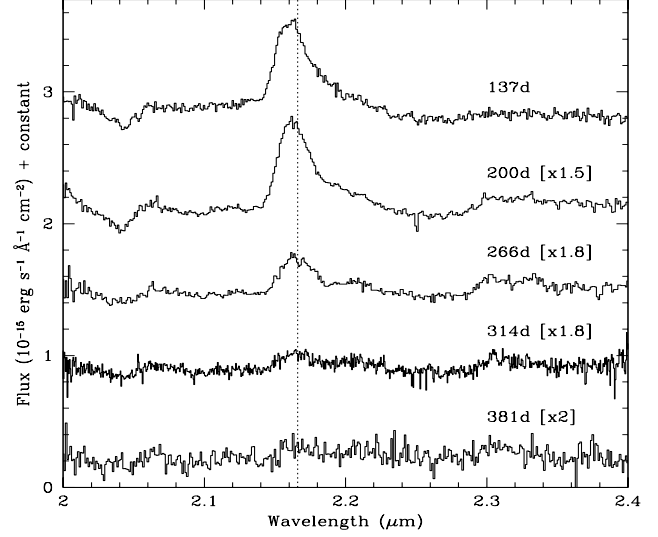


Figure 19. As in Fig. 17 but showing the evolution of the Brγ 2.166 μm emission line and of the CO emission in SN 2002hh.

ratio is expected for the 7291,7323 Å lines of the doublet (see Spyromilio, Stathakis & Meurer 1993), which may explain most of the extended red wing. In addition, as inferred for SN 1987A (see Spyromilio et al. 1991), both [Fe II] 7388,7452 Å and [Ni II] 7379,7413 Å may be contributing to the red wing.

The Hα peak exhibits a blueshift (w.r.t the adopted +110 km s⁻¹ centre-of-mass redshift) of -915 ± 30 km s⁻¹ at 162 d declining to -430 ± 30 km s⁻¹ at 397 d (see Table 10 and Fig. 14). (An even larger blueshift, ~ -1700 km s⁻¹, is seen at the photospheric epoch of 44 d). The Paβ line peak exhibits a blueshift of $\sim -200 \pm 100$ km s⁻¹ at 137 d but by 200 d this has increased to -700 ± 100 km s⁻¹. A similar shift is seen at 266 d, after which the shift reverts to around -200 ± 100 km s⁻¹ again. Brγ shows an unchanging

Table 10. Optical and infrared FWHM emission-line velocity widths and shifts.

Optical line velocity widths, [shifts] ^a (km s ⁻¹)				
	Epoch (days)			
Feature	162	227	250	397
H α	4530, [-915]	4475, [-805]	4475, [-750]	4630, [-430]
Infrared line velocity widths, [shifts] (km s ⁻¹)				
	Epoch (days)			
Feature	137	200	266	314
O I	3565, [-530]	3295, [-530]	2750, [+50]	2470, [-400]
Pa β ^b	3830, [-235]	4115, [-700]	4285, [-700]	3865, [-235]
Mg I	3890, [-300]	3530, [+400]	2820, [+800]	1940, [+600]
Br γ	4350, [-555]	3840, [-555]	3915, [-555]	-

^a Associated uncertainties are ± 180 km s⁻¹ for the velocity widths, and ± 30 and ± 100 km s⁻¹ for the optical and IR line shifts respectively.

^b Pa α is blueshifted by about -250 km s⁻¹.

blueshift of about -550 ± 100 km s⁻¹ from 137 d to 266 d (see Fig. 19). O I 1.129 μ m (Fig. 17) emission line shows an almost constant blueshift of $\sim -500 \pm 100$ km s⁻¹ except at 266 d when it shows a redshift of about $+50 \pm 100$ km s⁻¹. In contrast, Mg I 1.503 μ m (Fig. 18) shows an early blueshift of $\sim -300 \pm 100$ km s⁻¹, but from 200–314 d is redshifted by $\sim +600$ km s⁻¹.

The pattern of emission line blueshifts is probably indicative of variations in relative abundancies and conditions across the ejecta. However, apart from Pa β , no lines show evidence of an *increasing* blueshift with time nor progressive attenuation of the red wing, suggesting that, up to 381 d, there was no significant dust condensation in the ejecta.

5 SPECTROSCOPIC COMPARISON OF SN 2002HH AND SN 1987A

We now compare near-coeval late-time optical and NIR spectra for SN 2002hh and SN 1987A during the period of 4.5 months to ~ 1 year (see Figs. 20–24). The excellent late-time spectroscopic coverage of SN 2002hh means that it is the first CCSN for which such a comparison is possible. This comparison can be justified at the outset since, as we have shown, the nebular phase light curves of the two supernovae are quite similar and were powered by a similar amount of ⁵⁶Ni. Only at early times do the light curves differ significantly, primarily due to the different physical sizes of their progenitor stars (see Woosley 1988). In all the comparison figures the spectra have been corrected for redshift and extinction. The recession velocities are $+283$ and $+110$ km s⁻¹ for SN 1987A and SN 2002hh respectively. The dereddening made use of the extinction law of Cardelli et al. (1989). For SN 1987A we adopted $A_V = 0.6$ mag and $R_V = 3.1$. For SN 2002hh, we used the two-component extinction model ($A_{V1} = 3.3$ mag, $R_{V1} = 3.1$; $A_{V2} = 1.9$ mag, $R_{V2} = 1.1$)

(see Section 3). In addition, the SN 1987A spectra have been scaled to the distance of SN 2002hh (5.9 Mpc).

5.1 Optical spectra

In Figure 20 we compare optical spectra of SN 2002hh at epochs of 162 d, 250 d and 397 d with near-coeval spectra of SN 1987A. The SN 1987A spectra are from Spyromilio et al. (1991) and Stathakis (1996). The overall spectral form and evolution of the two SNe are rather similar, especially at 162 d and 250 d. At all three epochs the H α luminosity is similar between the two SNe. The Na I D P Cygni feature is also similar in the two events. The most striking difference between the two SNe is that both [Ca II] 7291,7323 Å and the Ca II IR triplet are much stronger in SN 1987A throughout the 162–397 d period. Moreover the strong Ca I 1.99 μ m feature in SN 1987A at 192 d is virtually absent in the SN 2002hh 200 d spectrum (see following section). We infer a significantly lower calcium abundance in SN 2002hh.

At 162 d and 397 d the SN 2002hh optical continuum is distinctly bluer than that of SN 1987A while at 250 d they are about the same. At 162 d the flux levels toward the blue are similar, but by 1 μ m the SN 1987A continuum flux exceeds that of SN 2002hh by more than $\times 2$. Comparison of the overlap of the red end of the 162 d optical spectrum with the blue end of the 137 d and 200 d infrared spectra of SN 2002hh suggests that some of the 02hh/87A red discrepancy ($\sim \times 1.35$) is due to error in the linear flux correction function (see Section 2.3) for the 162 d SN 2002hh optical spectrum. At least some of the remaining discrepancy may be due to error in the SN 1987A fluxing. Unfortunately we are unable to apply an overlap test here since there is a 0.12 μ m gap between the SN 1987A optical and IR spectra. In the 397 d optical spectrum of SN 2002hh, the continuum flux towards the red agrees well with that of SN 1987A at 371 d. However, as we move to the blue we see a growing excess in the SN 2002hh continuum relative to that of SN 1987A. We were unable to check the spectral fluxing of SN 2002hh against photometry for the 397 d optical or 381 d IR spectra, but nevertheless we find a fair flux agreement in the small optical/IR overlap region around 0.94 μ m. This gives us confidence that the fluxing towards the red end of the SN 2002hh optical spectrum is good. However, it is possible that at least some of the blue discrepancy could be due to fluxing error which increases towards shorter wavelengths (see Section 2.3). Another possibility is the presence of uncorrected background contamination as Milne & Wells (2003) concluded was the case for the Type Ia SN 1989B. A third explanation is that in SN 2002hh a small fraction of the peak luminosity is being scattered by circumstellar or interstellar dust. Thus, as the supernova flux fades between 162 d and 397 d, the relative contribution of the scattered light increases. Dust echo-enhancement of late-time optical spectra has been reported for the Type Ia SNe 1991T and 1998bu (Patat 2005 and references therein). Spectral modelling of the blue excess may distinguish between these possibilities for SN 2002hh. However, we are much less persuaded that the blue continuum is due to ejecta-CSM interaction since no signs of this are seen in the contemporary spectral lines.

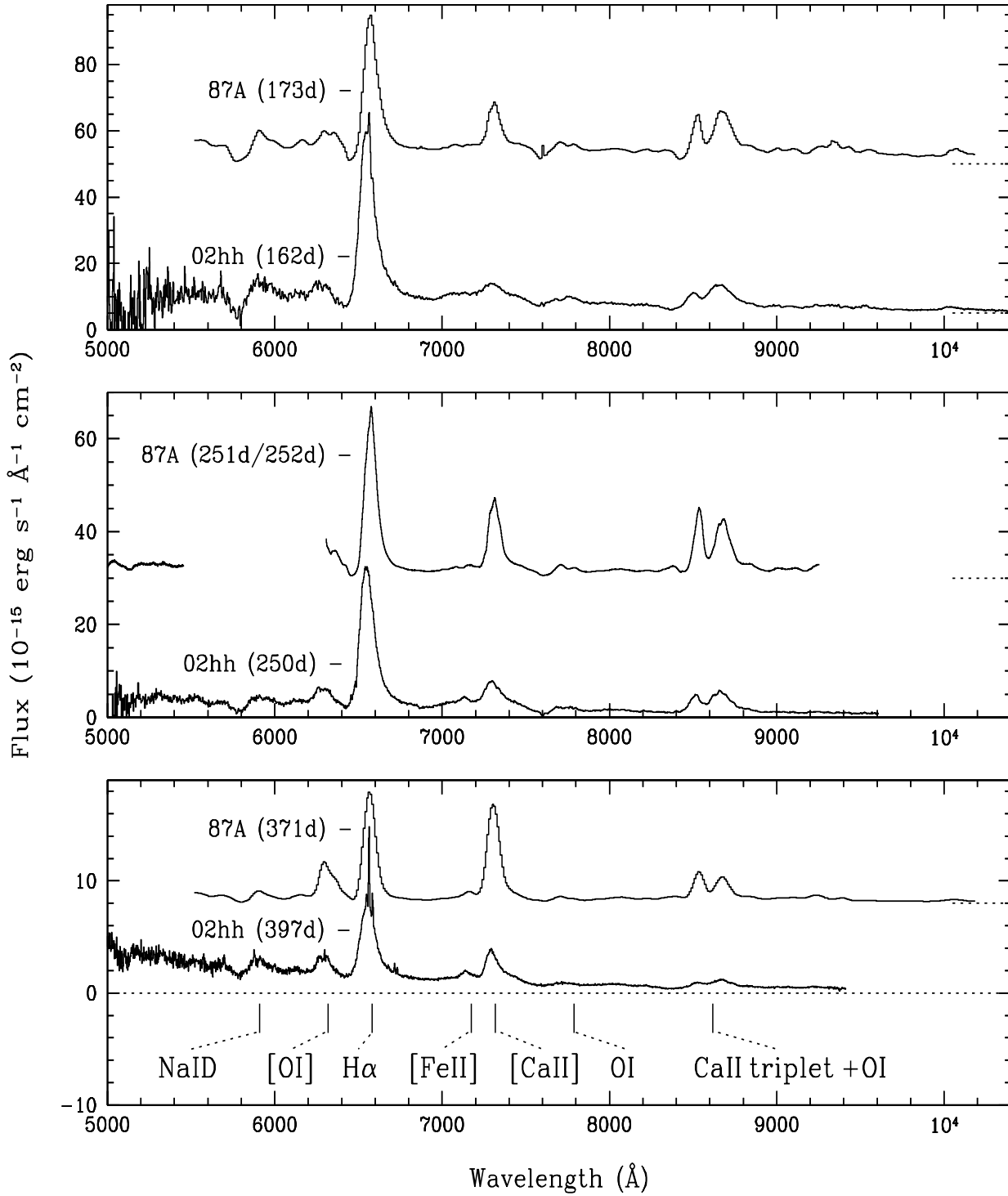


Figure 20. Comparison of the optical spectra of SN 2002hh with near-coeval spectra of SN 1987A. The spectra have been corrected for redshift and extinction. The SN 1987A spectra have been scaled to the distance of SN 2002hh (5.9 Mpc) and displaced vertically for clarity. At the bottom we show the line identifications for SN 1987A as given in Spyromilio et al. (1991).

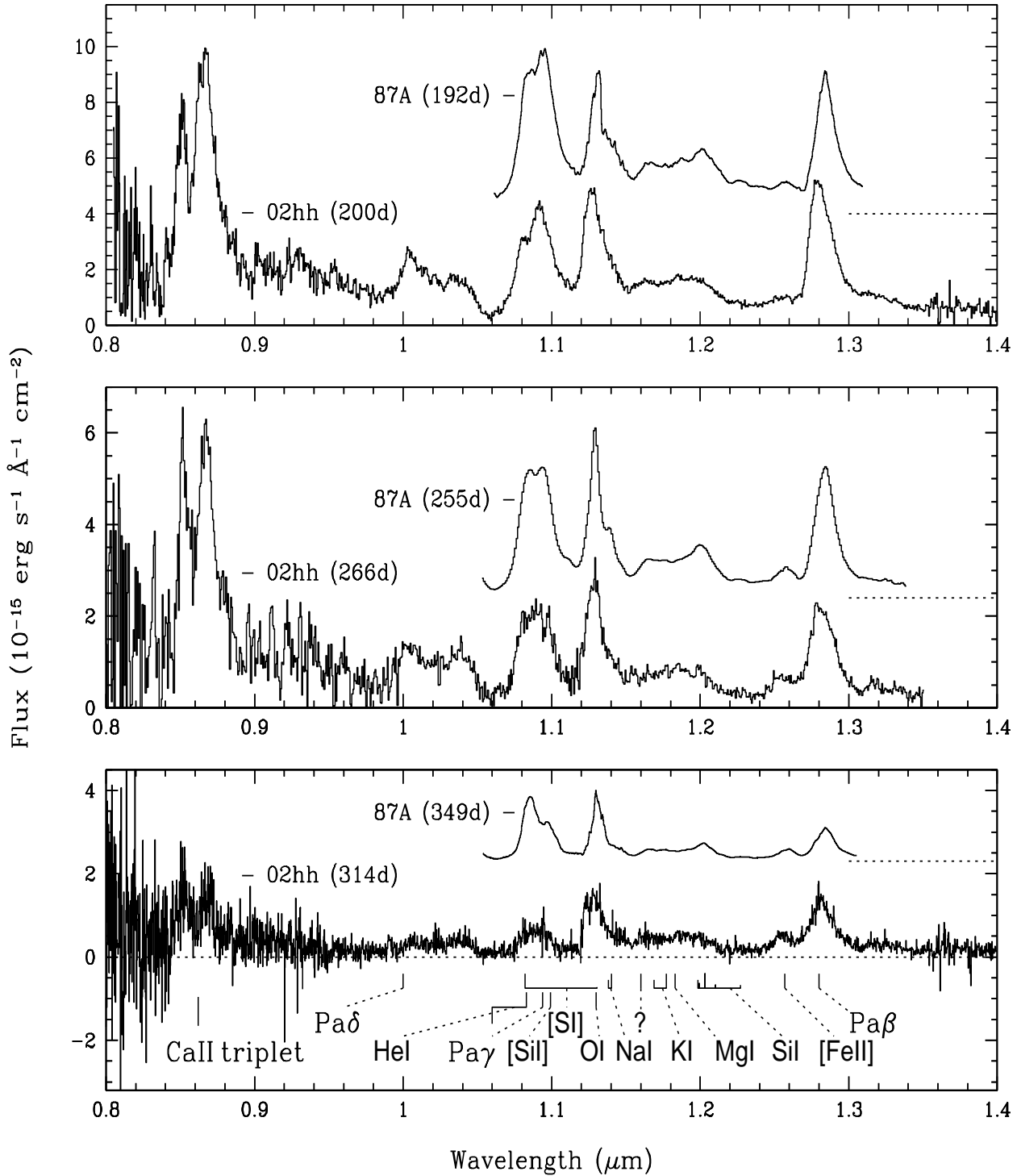


Figure 21. Comparison of the NIR spectra of SN 2002hh with near-coeval spectra of SN 1987A in the J-band (0.8–1.4 μm) region. The spectra have been corrected for redshift and extinction. The SN 1987A spectra have been scaled to the distance of SN 2002hh (5.9 Mpc) and displaced vertically for clarity. At the bottom we show the line identifications for SN 1987A as given in Meikle et al. (1993).

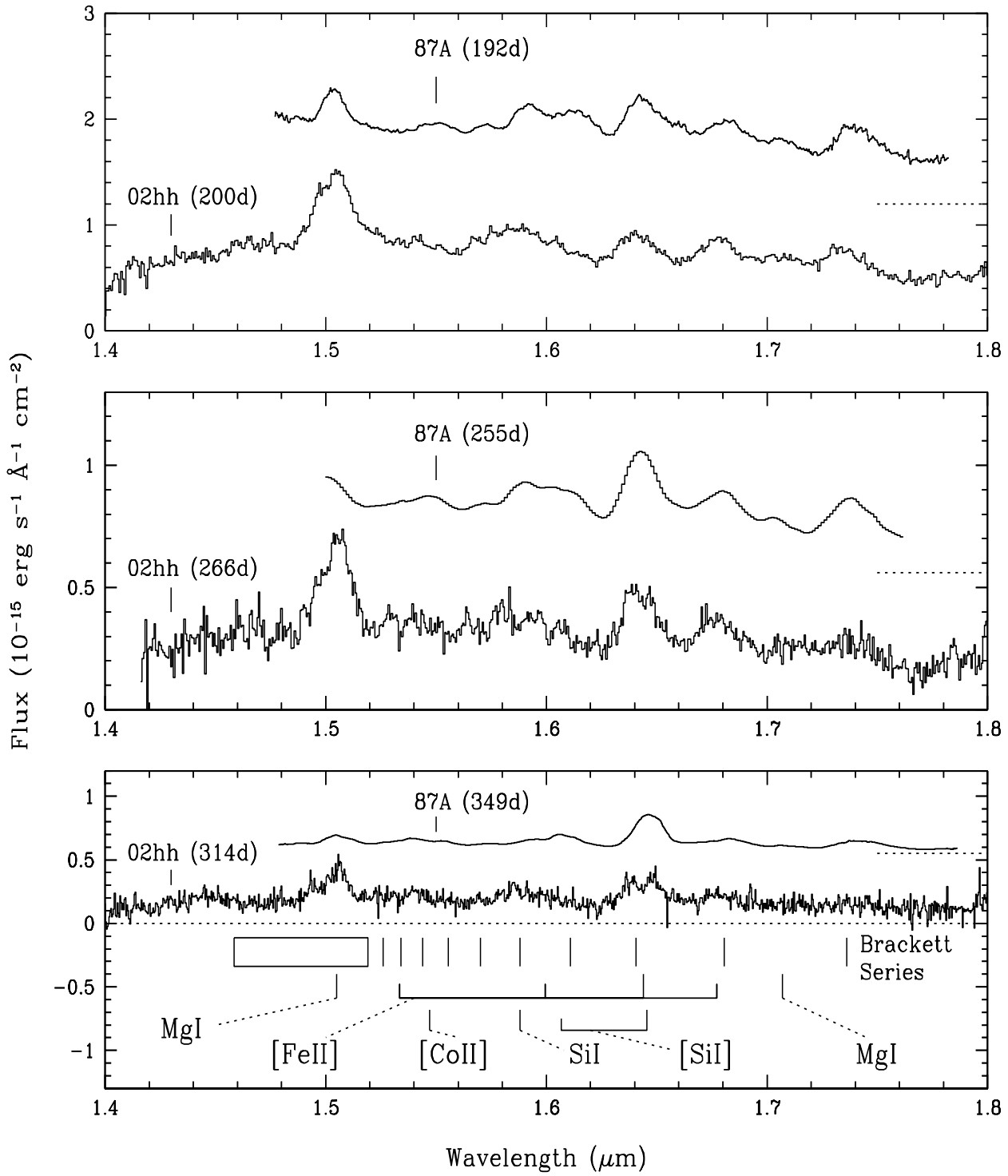


Figure 22. As for Fig. 21, but for the H-band (1.4–1.8 μm) region.

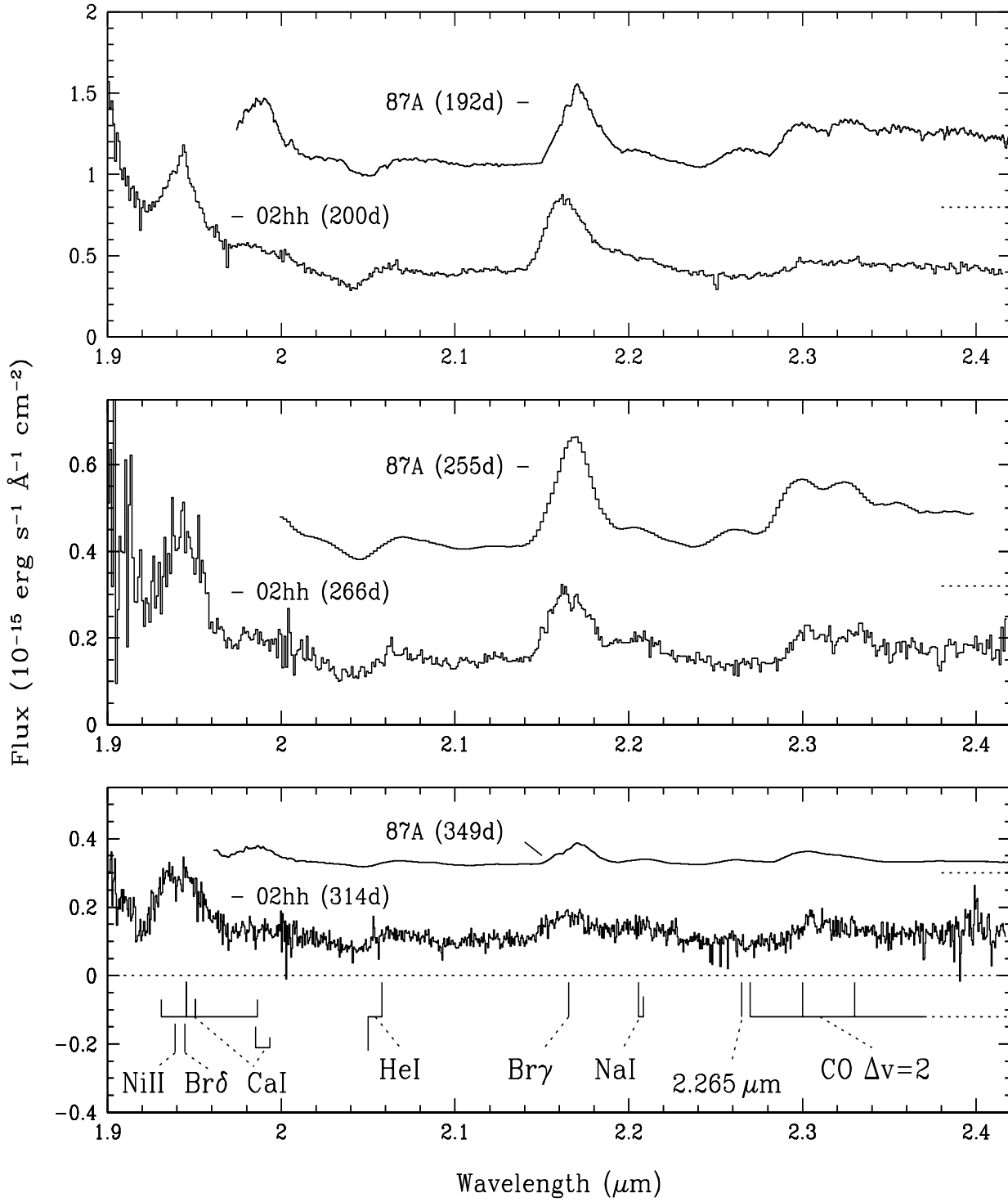


Figure 23. As for Fig. 21, but for the K-band (1.9–2.4 μm) region.

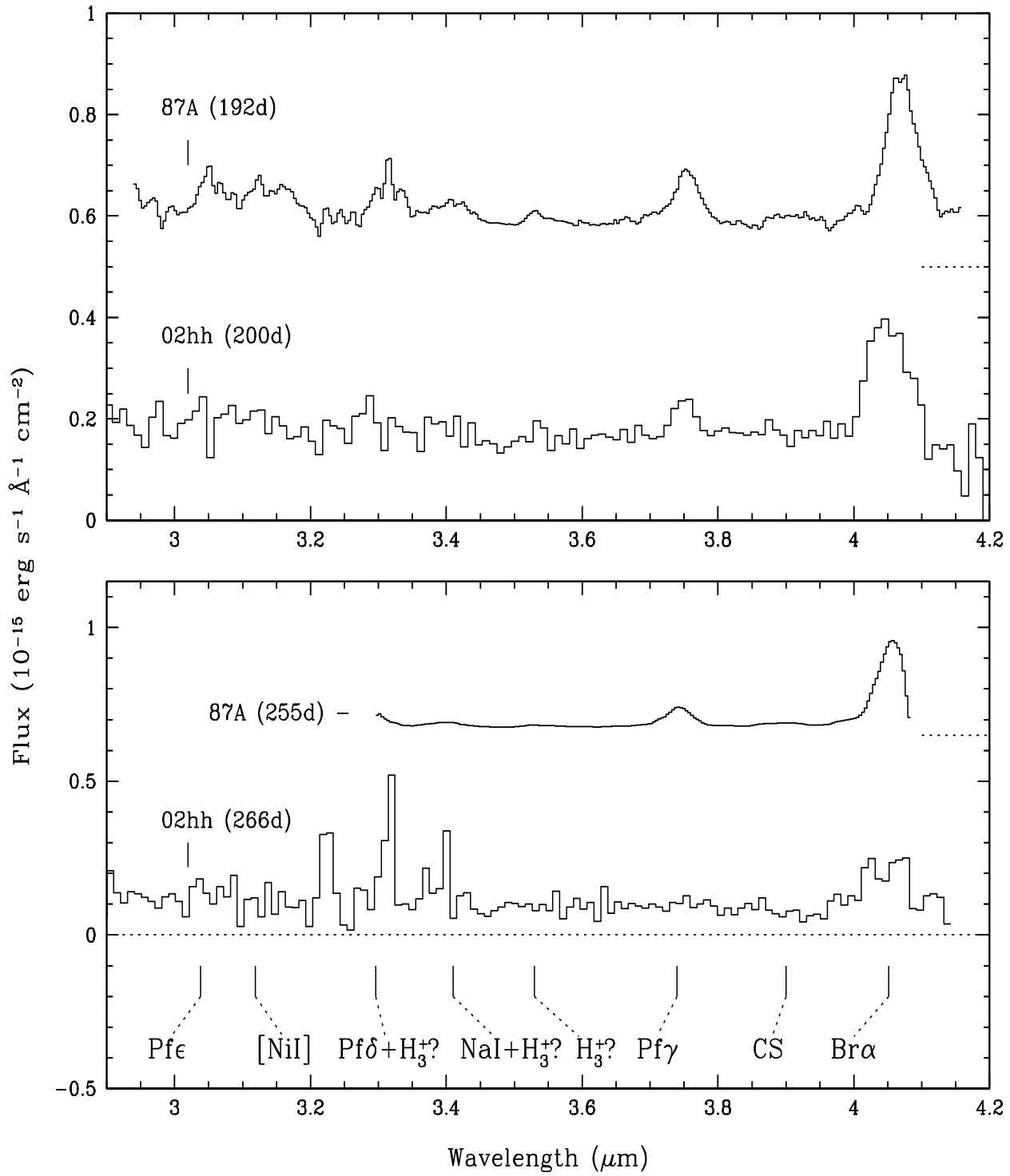


Figure 24. As for Fig. 21, but for the L-band ($2.9\text{--}4.2 \mu\text{m}$) region.

5.2 Near-IR spectra

In Figures 21 to 24, we compare $\sim 0.8\text{--}4.2\ \mu\text{m}$ spectra of SN 2002hh at 200 d, 266 d and 314 d with near-coeval spectra of SN 1987A taken from Meikle et al. (1989). At the bottom of each figure we show the line identifications for SN 1987A as given in Meikle et al. (1993). The fluxing for SN 1987A has been revised to match the IR photometry of Bouchet & Danziger (1993), Catchpole et al. (1987, 1988) and Whitelock et al. (1988). In particular, the L' band spectra of SN 1987A at 192 d and 255 d have been scaled by $\times 1.31$ and 1.46 respectively. In addition, the SN 1987A fluxes have been scaled to 5.9 Mpc, the distance of SN 2002hh. All the SNe 1987A and 2002hh spectra have been dereddened as described earlier.

As in the optical region, the spectral form and evolution of the two SNe are very similar. The similarity of the form and fluxes of the spectra in the *J* and *H* bands is particularly impressive especially when one considers that the only corrections have been to the extinction and the difference in distance.

J-band spectra

The $\text{Pa}\gamma\ 1.094\ \mu\text{m}$ -He I $1.083\ \mu\text{m}$ blend is stronger in SN 1987A, especially by 314 d and yet the He I absorption remains similar between the two SNe (although this could simply be due to saturation). The $\text{Pa}\beta\ 1.282\ \mu\text{m}$ and O I $1.129\ \mu\text{m}$ emission peaks are at about the same level in both events throughout the 200–314 d period. The [Fe II] $1.257\ \mu\text{m}$ is about the same in both SNe up to 266 d, but at 314 d it is about twice as strong in SN 2002hh than in SN 1987A. The Si I $1.20\ \mu\text{m}$ emission is somewhat stronger in SN 1987A, but this difference fades with time. Some of the $\text{Pa}\gamma\ 1.094\ \mu\text{m}$ -He I $1.083\ \mu\text{m}$ blend difference may be due to the additional presence of [Si I] $1.099\ \mu\text{m}$ at a stronger intensity in SN 1987A due to a higher abundance of silicon in this event. However, it seems unlikely that this can provide the whole explanation for the difference.

H-band spectra

The overall appearance of the *H*-band spectra is similar between the two SNe. The most striking and persistent difference is the factor of $\times 2.5$ greater luminosity of Mg I $1.503\ \mu\text{m}$ in SN 2002hh. Redward of the Mg I line some other differences are seen between the two events. SN 1987A shows a persistent emission feature at $1.61\ \mu\text{m}$ which is virtually absent from SN 2002hh. Meikle et al. (1989) ascribed the $1.61\ \mu\text{m}$ emission to [Si I] $1.6068\ \mu\text{m}$. The weakness of the corresponding emission in SN 2002hh suggests a lower silicon abundance in this SN. Interestingly, the $1.64\ \mu\text{m}$ feature is comparable to, or slightly stronger than in SN 1987A during the 200–314 d period. Meikle et al. (1989) attribute this feature to a blend of [Fe II] $1.644\ \mu\text{m}$, [Si I] $1.645\ \mu\text{m}$ and Br12. However the weakness of the [Si I] $1.6068\ \mu\text{m}$ component in SN 2002hh suggests that the $1.64\ \mu\text{m}$ feature is predominantly due to iron and hydrogen in this SN.

K-band spectra

The two SNe show very similar features from 200 d to 314 d, although no comparison can be made shortward of about $1.97\ \mu\text{m}$ where the SN 1987A data terminates. The peak-base intensity of $\text{Br}\gamma\ 2.166\ \mu\text{m}$ is similar at 200 d, at 266 d it is stronger in SN 1987A, but by 314 d it is stronger in SN 2002hh. The He I $2.058\ \mu\text{m}$ feature is of comparable strength at ~ 200 d in both SNe, but is stronger in SN 2002hh thereafter. The Na I $2.206\ \mu\text{m}$ which shows up in both SNe on the red wing of the $\text{Br}\gamma$ line at ~ 200 d is increasingly prominent in SN 2002hh at later epochs. The CO first overtone is about a factor of $\times 3$ stronger in SN 1987A at 192 d than in SN 2002hh. However, the SN 1987A CO intensity fades more rapidly than in SN 2002hh so that by 314 d the situation is reversed. Indeed, by 381 d the SN 2002hh CO emission appears to be about $\times 2$ stronger than in SN 1987A (see below). There is little sign of the unidentified $2.265\ \mu\text{m}$ feature in SN 2002hh (see below). In addition, the strong Ca I $1.99\ \mu\text{m}$ feature in SN 1987A at 192 d is virtually absent in the SN 2002hh 200 d spectrum. A striking difference between the two SNe is that SN 2002hh shows a much stronger underlying continuum. At 200 d, the excess continuum amounts to $\sim 1.4 \times 10^{-16}\ \text{erg s}^{-1}\ \text{cm}^{-2}\ \text{\AA}^{-1}$ falling to about half this value at 266 d and maintaining this level until 314 d. The (SN 2002hh):(SN 1987A) continuum ratio rises from 1.6 to 3.6 between 200 d and 314 d. The continuum is discussed below.

L-band spectra

In spite of the lower S/N of the SN 2002hh spectra, we can see that $\text{Br}\alpha$ and $\text{P}\gamma$ have a similar strength to SN 1987A at 200 d. By 266 d $\text{Br}\alpha$ is still of roughly comparable strength between the two SNe, but there is no longer any sign of $\text{P}\gamma$ in SN 2002hh. As in the *K*-band, a striking aspect of the *L*-band spectrum is the much stronger continuum in SN 2002hh. The (SN 2002hh):(SN 1987A) continuum ratios in the *L*-band are similar to those seen in the *K*-band, *viz.* 1.8 at 200 d and 3.6 at 266 d. The continuum is discussed below.

5.2.1 Carbon monoxide

In Figures 25–28 we compare the CO first overtone emission spectra of SNe 1987A and 2002hh. The SN 1987A spectra have been scaled to the distance of SN 2002hh. In addition, in order to effect a better comparison between the two supernovae, the SN 1987A spectra have been displaced vertically so that the underlying continuum (judged from the spectrum to the blue of the CO emission) matches that of SN 2002hh. The excess continuum in SN 2002hh is discussed below. Both spectra in each figure have been corrected for extinction and redshift. In Fig. 25 we compare the 137 d spectrum of SN 2002hh with the 110 d spectrum of SN 1987A. In both cases CO emission is barely visible. In Fig. 26 we compare the 200 d spectrum of SN 2002hh with the 192 d spectrum of SN 1987A. First overtone emission is clearly present in both spectra, but is significantly weaker in SN 2002hh. The unidentified $2.265\ \mu\text{m}$ feature prominent in SN 1987A is completely absent in SN 2002hh (see below). While the relative weakness of the SN 2002hh CO emission persists to 266 d (Fig. 27) the supernovae exhibit a similar relative decline in the P branch ($\sim 2.37\ \mu\text{m}$). LTE modelling

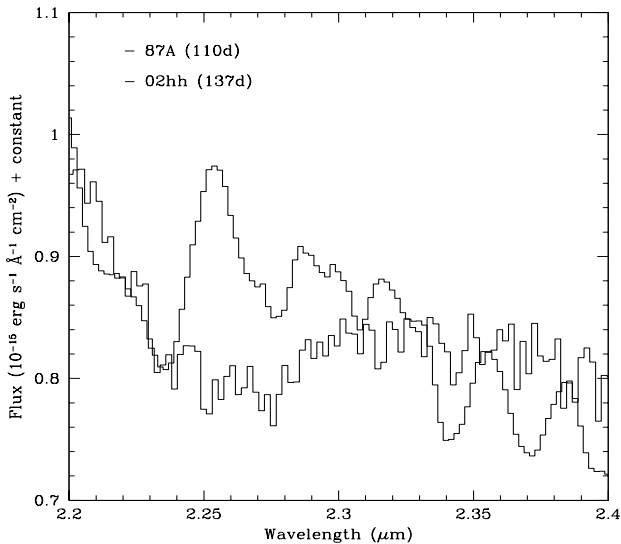


Figure 25. Comparison of the first-overtone CO profiles of SN 2002hh at 137 d with that of SN 1987A at 110 d. The SN 1987A spectrum has been scaled to the distance of SN 2002hh, and has been displaced vertically so that the underlying continuum matches that of SN 2002hh (see text). The spectra have been corrected for redshift and extinction.

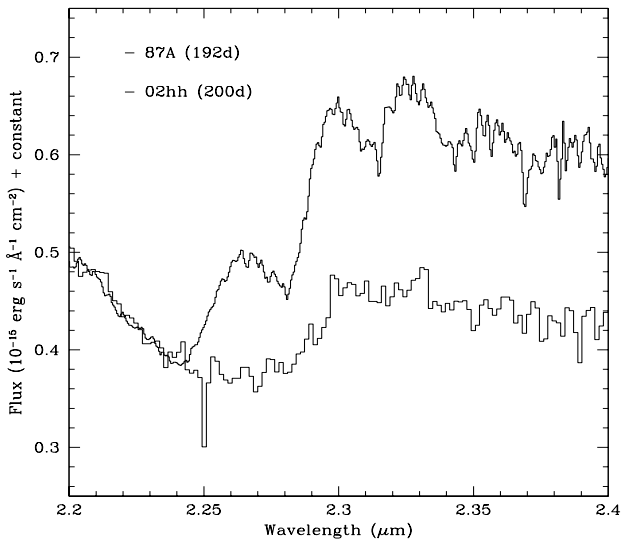


Figure 26. As for Fig. 25 but for SN 2002hh at 200 d and SN 1987A at 192 d.

of the CO emission profile in SN 1987A (e.g. Spyromilio et al. 1988) showed that by 255 d the decline in the P branch ($\sim 2.37 \mu\text{m}$) flux implies that the temperature of the CO emitting region had fallen below 2000 K. We conclude that similar cooling took place in SN 2002hh. This is important as it suggests that some regions of the ejecta may cool sufficiently for dust condensation to take place. A quasi-periodic structure is produced by the R-branch bandheads of the 0–2, 1–3, 2–4 etc. vibrational transitions. The visibility of this structure in the 266d SN 2002hh spectrum is similar to that of SN 1987A at 255 d, implying a similar CO velocity $1800\text{--}2000 \text{ km s}^{-1}$.

In Figure 28, we compare the CO spectrum of SN 1987A

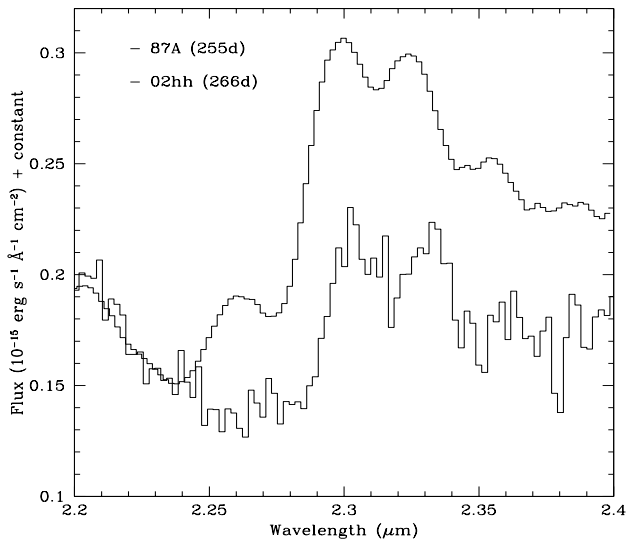


Figure 27. As for Fig. 25 but for SN 2002hh at 266 d and SN 1987A at 255 d.

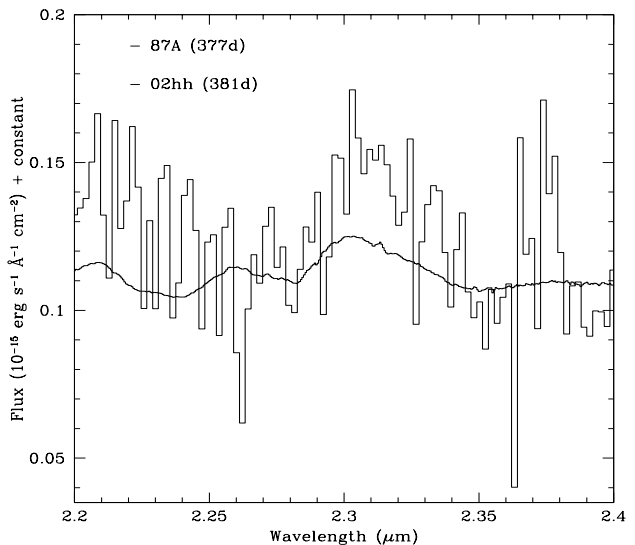


Figure 28. As for Fig. 25 but for SN 2002hh at 381 d and SN 1987A at 377 d.

at 377 d with that of SN 2002hh at 381 d. In spite of the very low S/N of the latter, it seems that by this epoch the R-branch intensity of SN 2002hh was about $\times 2$ stronger than in SN 1987A.

5.3 The unidentified 2.265 μm feature

An emission feature at $2.265 \mu\text{m}$ is present in the spectra of SN 1987A from as early as 192 d to at least 2 years post-explosion. Spyromilio, Leibundgut & Gilmozzi (2001) also claim detection of this feature in the Type IIP SN 1999em at ~ 170 d, albeit at a much lower S/N. However, in other CCSNe *K*-band spectra the feature is at best marginally present (SN 1996ad (105 d) - Spyromilio & Leibundgut 1996; SN 1998dl (~ 150 d) - Spyromilio et al. 2001) or absent (SN 1998S (109 d) - Fassia et al. 2001; SN 1999gi (126 d), SN 2000ew (97 d)- Gerardy et al. 2002). It might be in-

ferred from this that the $2.265 \mu\text{m}$ feature is actually quite ubiquitous, but does not strongly appear until after ~ 150 d. However, our SN 2002hh observations (see Figs. 25–28) show that the feature was certainly absent up to 200 d and, perhaps, even up to 266 d. While the origin of this feature has been debated for many years (Spyromilio et al. 1988; Meikle et al. 1993; Liu & Dalgarno 1995; Spyromilio & Leibundgut 1996; Gearhart, Wheeler & Swartz 1999; Gerardy et al. 2000, 2002; Spyromilio et al. 2001) we must conclude that as yet there is no consensus as to its true identity nor why it seems to exhibit such a large range of intensities from one supernova event to another.

5.4 The late-time near-IR continuum

As already mentioned, one of the most notable differences between the late-time coeval NIR spectra of SNe 1987A and 2002hh is the much stronger KL continuum in the latter event. This was illustrated for epochs 200 d and 266 d, for which both K and L band spectra were available. Inspection of Figs. 23 and 24 show that this excess in SN 2002hh probably persisted to beyond 314 d. We would like to understand the origin of this continuum, and in particular, why it is so much stronger than in SN 1987A.

In SN 1987A, Meikle et al. (1993) found that the late-time JHK continuum could be well represented by a $\lambda^{-2.5}$ -law between 192 and 574 days. They found that this continuum was several times stronger than would be expected from optically-thin, ionised hydrogen, as well as having a steeper spectrum than that of pure free-free emission. They suggested that the JHK continuum was due to a mixture of emission from optically thick and optically thin gas, comprising many contributing species and subject to spatial variations in temperature and ionisation. Different behaviour was seen in the L -band continuum. While the $\lambda^{-2.5}$ -law provided a fair representation of the 192 d continuum to about $3.65 \mu\text{m}$, at longer wavelengths the slope flattened. Moreover, by 349 d, the break in slope had moved back to $\sim 3.3 \mu\text{m}$. Meikle et al. found that between 192 d and 349 d the L -continuum faded at the same rate as did the CO first overtone emission in the K -band. They therefore suggested that the excess L -band continuum was caused by a blend of unidentified molecular emission bands.

Wooden (1989) (see also Wooden et al. 1993 and Wooden 1997) hypothesized that at 60 and 260 d, part of the $3\text{--}12 \mu\text{m}$ continuum of SN 1987A was due to warm dust in the circumstellar environment, heated by the early-time luminosity i.e. an IR-echo. She derived dust temperatures of $\sim 1300\text{--}1600$ K at 60 d, falling to $\sim 560\text{--}700$ K at 260 d, and suggested that the dust lay in the circumstellar ring (Wooden 1997). However, as Meikle et al. (1993) point out, the Wooden dust model does not account for much of the L -band continuum which appears to be in *excess* of the Wooden dust model spectra. Nevertheless, even if we accept the Meikle et al. “blended molecular bands” hypothesis for SN 1987A, it is not clear that this solution can be extended to the significantly larger continuum excess in SN 2002hh. Two points argue against doing so. One is that there is convincing evidence that the excess is at least as strong in the K window, where strong, blended and unidentified molecu-

lar emission is perhaps less likely. The other point is that, if we attribute all of the SN 2002hh continuum to molecular emission, then why is the CO emission so much *weaker* than in SN 1987A, at least for epochs 200 d and 266 d? We are therefore persuaded to look at the possibility that at least some of the excess continuum in SN 2002hh is due to warm dust.

Comparison of the SN 2002hh $1\text{--}4 \mu\text{m}$ spectra with blackbody functions shows that much of the excess continuum in the K and L windows could be reproduced with blackbodies at $1100\text{--}1300$ K and having an expansion velocity of $\sim 1700 \text{ km s}^{-1}$. Such temperatures and velocities may be consistent with an origin in newly condensing dust or in an IR echo. However the presence of the KL spectral excess as early as 200 d plus the rather high blackbody temperature tends to argue against the condensing dust hypothesis. In addition, the 200 d CO emission is a factor of $\times 3$ weaker in SN 2002hh than in SN 1987A, further reducing the prospect that sufficiently cold dust-forming conditions might have occurred around this epoch. The alternative possibility is that much of the excess could have been due to an IR echo from pre-existing dust in the progenitor CSM. We have therefore constructed an IR-echo model and have used this to explore the parameters of a dusty CSM that could produce an echo of about the right spectral shape and intensity to account for the excess.

The IR-echo model follows those of Bode & Evans (1980), Dwek (1983) and Graham & Meikle (1986). The input UV-optical luminosity is a parameterised version of the SN 1999em bolometric lightcurve of Elmhamdi et al. (2003) scaled to the Cepheid distance of 11.7 Mpc (Leonard et al. 2003) *viz.* $27.4 \times 10^{41} e^{-t(d)/18.7} \text{ ergs s}^{-1}$ to 24 days, $10.6 \times 10^{41} e^{-t(d)/171} \text{ ergs s}^{-1}$ for 24–118 days, and $3.06 \times 10^{41} e^{-t(d)/130} \text{ ergs s}^{-1}$ thereafter. A grain absorptivity of 1 was assumed. The dust grain size was $0.05 \mu\text{m}$, the grain material density was 3 gm cm^{-3} and the grain number density at 6700 A.U. was $9 \times 10^{-9} \text{ cm}^{-3}$ with an r^{-2} (steady wind) dependence. The resulting optical depth to the input UV-optical luminosity was $\tau = 0.09$. A dust grain emissivity proportional λ^{-2} was assumed for the IR emission. The evaporated dust-free cavity was $R_v = 5000 \text{ A.U.}$ This was obtained by scaling from the SN 1979C value (Dwek 1983) assuming $r_v \propto L_{peak}^{0.5}$ (Dwek 1985). The paraboloid corresponding to the peak SN luminosity lay beyond the dust-free cavity at all three epochs. The CSM outer radius was 133,000 A.U. and the distance of SN 2002hh was 5.9 Mpc. The derived vertex dust temperatures were 1085 K, 975 K and 925 K on days 200, 266 and 314 respectively. The total mass of dust is $1.6 \times 10^{-3} M_{\odot}$. Assuming a standard grain-to-gas ratio (by mass) of 0.006, the corresponding CSM mass was $0.27 M_{\odot}$, or $0.28 M_{\odot}$ if we include the gas in the dust-free cavity.

In Fig. 29 we compare the IR echo model spectra with the observed KL spectra for 200 d, 266 d and 314 d. In the last case, no L -band spectrum was available and so we show the corresponding L' photometry point instead. We conclude that much of the KL excess can be reproduced with a CSM mass of $\sim 0.3 M_{\odot}$. Only small optical depth (~ 0.1) is required to reproduce the KL -excess. In Section 3.2 we ob-

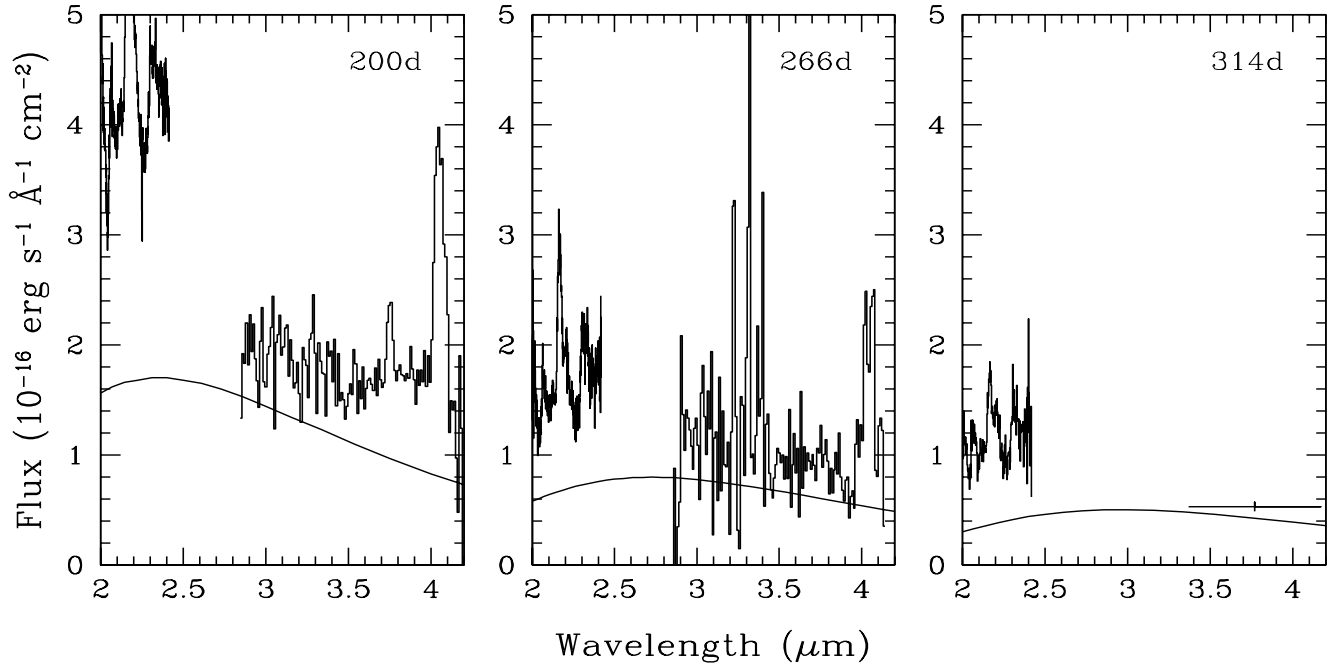


Figure 29. Infrared spectra of SN 2002hh compared with IR-echo model spectra for three epochs, illustrating that much of the KL excess could be due to an IR-echo (see text for details of model). No L -band spectrum was available for 314 d and so we show the corresponding L' photometry point instead.

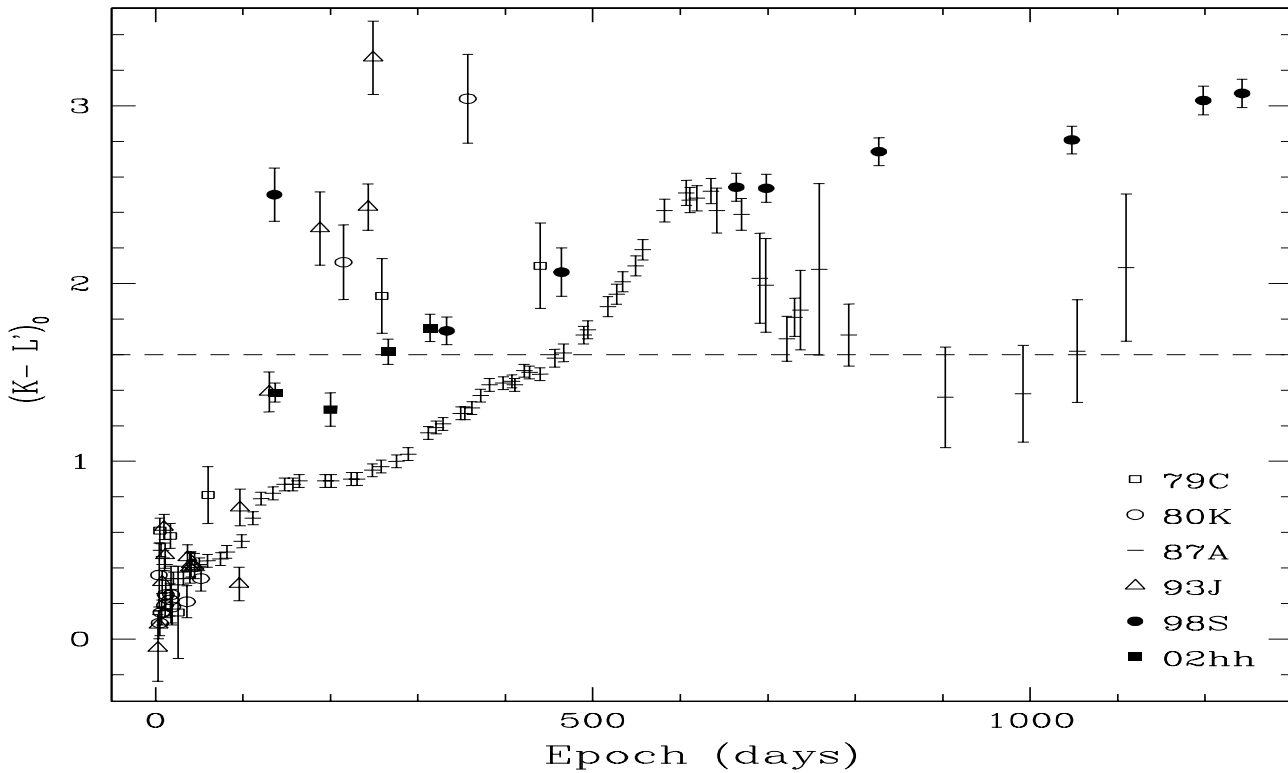


Figure 30. The temporal evolution of the extinction-corrected colour $(K - L')_0$ for core-collapse supernovae, including SN 2002hh (filled squares). The epoch gives the approximate number of days since outburst. Pozzo et al. (2004), suggested that colours lying above the dashed line at $(K - L')_0 = 1.6$ indicate a contribution to the IR emission from hot dust. The $(K - L')_0$ colour of SN 2002hh is redder than that of SN 1987A by about 0.5 mag, although the temporal trend is similar. However, even the latest SN 2002hh point lies only slightly above the $K - L' = 1.6$ line and so barely provides support for dust condensation.

tained $A_V = 1.9$ mag, i.e. $\tau_V = 1.6$ for the “dust pocket”. We conclude that most of the dust-pocket extinction occurred well beyond the progenitor CSM.

Pozzo et al. (2004) suggested that if the $K - L'$ colour of a CCSN exceeds ~ 1.6 within a year after explosion it indicates the presence of circumstellar dust heated by the supernova’s early-time luminosity (i.e. an “IR echo”), although there may also be a contribution from newly-condensed dust in the ejecta. In Fig. 30 we update Fig. 15 of Pozzo et al. where we plot the $K - L'$ evolution of SN 2002hh compared with other CCSNe. Even the latest SN 2002hh point lies only slightly above the $K - L' = 1.6$ line. We therefore conclude that the $K - L'$ analysis does not provide additional support for either hypothesis. As indicated in Section 4.1.4, the line profile behaviour up to 381 d also yields no evidence for dust condensation in the ejecta.

The lack of evidence for dust condensation during the first year does not rule out the possibility of grain formation at later epochs. Dust formation happened only after the elapse of one year in SN 1987A, SN 1998S and SN 1999em. Moreover, Meikle et al. (2005a,b and in preparation; see also next Section) have presented mid-IR evidence for dust condensation in the ejecta of SN 2002hh by 590 d, close to the condensation epoch of SN 1987A.

6 CONCLUSIONS

We have presented optical/IR photometric and spectroscopic observations of SN 2002hh covering a period of ~ 400 days during the photospheric and nebular phases. We confirm it to be a normal Type IIP event. We show the first-ever L -band spectra for such an event. The only other supernova for which L -band spectra have been obtained was the peculiar (and very close) Type II SN 1987A. SN 2002hh is one of the most highly-extinguished supernovae ever investigated. By assuming a similar early-time spectroscopic behaviour to the well-studied “template” Type IIP SN 1999em, we first derived a total extinction of $A_V = 5.2$ mag. This value was checked against the K I 7699 Å absorption line, from which we infer A_V values of 1.55 and 1.77 mag ($R_V = 3.1$) in the H I ISMs of the Milky Way and NGC 6946 respectively. This suggests that there is an additional $A_V = 1.9$ mag of extinction which is not traced by the K I absorption line. However, we find that a good match between coeval early-time spectra of SNe 1999em and 2002hh is obtainable using a 2-component extinction model for SN 2002hh, with $A_V = 3.3$ mag and $R_V = 3.1$ (Component 1), and $A_V = 1.9$ mag with $R_V = 1.1$ (Component 2). An R_V value as low as 0.7 has been invoked in the past in multi-component extinction models (see Wang et al. 2004 and refs. therein) and probably implies a distinct line-of-sight “dust pocket” where the mean dust grain size is smaller than in the H I ISM. We suggest that this dust pocket may be associated with the H II region and dust lane which lies close to the SN 2002hh line-of-sight. We do *not* associate most of the second extinction component with either newly-condensed dust or the progenitor CSM (see below).

The early-time optical light curves of SNe 1999em and

2002hh are generally well-matched, as are the radioactive tails of these two SNe and SN 1987A. This suggests a certain robustness in the adopted extinction in spite of it being derived using only one epoch of spectroscopic data. The late-time similarity of SN 2002hh to SN 1987A implies that $(0.07 \pm 0.02) M_\odot$ of ^{56}Ni was ejected by SN 2002hh. This is confirmed by our derivation of the *OIR* luminosity at 200 d and 266 d and by the similar coeval luminosities of the [Fe II] 1.257 μm line in SNe 1987A and 2002hh. In the nebular phase, however, the *HKL'* luminosities of SN 2002hh exhibit a growing excess with respect to those of SN 1987A. We attribute much of this excess to an IR-echo from a pre-existing, dusty CSM. The NIR light curves of SN 1999em are systematically fainter than those of SN 2002hh by about 0.6 mag. We suspect an error in the calibration of the SN 1999em magnitudes.

During the nebular phase, linewidths of around 3800–4600 km s^{-1} (FWHM) are seen in the hydrogen lines. There is weak evidence of a modest decline in the widths of the other lines with time. During the earlier part of the nebular phase both the Balmer and Paschen lines tend to be asymmetric with enhanced red wings. The presence of strong He I 1.083 μm emission as early as 137 d (Fig. 8(b)) implies upward mixing of radioactive iron-group elements (Graham 1988, Fassia et al. 1998, Fassia & Meikle 1999). [O I] 1.129 μm is also prominent during the nebular phase, indicating microscopic mixing of hydrogen and oxygen. Further evidence of mixing is provided by the profiles of [O I] 6300,64 Å and Mg I 1.503 μm which exhibit pronounced irregularities during the earlier part of the nebular phase. This suggests clumping in the SN ejecta as was inferred for SNe 1987A and 1993J (Matheson et al. 2000b and refs. therein). In contrast, the lack of well-defined small-scale structures in [Ca II] 7291,7323 Å points to a more uniform distribution in the SN ejecta.

Persistent blueshifts are seen in a number of prominent lines. The pattern of blueshifts is probably due to variations in relative abundancies and conditions across the ejecta. However, apart from Pa β , no lines show evidence of an *increasing* blueshift with time nor progressive attenuation of the red wing, suggesting that, up to 381 d, there was no significant dust condensation in the ejecta.

We have presented a detailed comparison of the late time optical and NIR spectra of SNe 1987A and 2002hh. While the overall impression is one of similarity between the spectra of the two events, there are notable differences. The Mg I 1.503 μm luminosity in SN 2002hh is much stronger while emission from silicon and calcium is much weaker. Yet, a number of pieces of evidence point to similar iron-group masses having been produced in the two events. The explosive nucleosynthesis models of Thielemann, Nomoto & Hashimoto (1996) suggest that the magnesium mass in particular is a sensitive indicator of progenitor mass, increasing by a factor of about $\times 15$ as we go from a progenitor mass of 13 M_\odot to 20 M_\odot . The same models also predict a silicon mass increase of $\times 2$ while the calcium abundance decreases slightly down to a progenitor mass of 15 M_\odot and then increases slowly thereafter. In contrast, due to the rising mass cut, the mass of ejected iron *falls* by a factor of about $\times 2$

over the same progenitor mass range. Clearly the overall abundance trend between SN 1987A and SN 2002hh is not consistent with the explosion model predictions. It appears that during the burning to intermediate-mass elements, the nucleosynthesis did not progress as far as might have been expected given the mass of iron ejected.

Elmhamdi et al. 2003 (and refs. therein) made use of the [O I] 6300,6364 Å doublet luminosity to place constraints on the progenitor mass of SN 1999em, by scaling from the [O I] luminosity and ^{56}Ni mass of SN 1987A. Following a similar procedure for SN 2002hh, at +397 d the coeval [O I] doublet luminosity is about $\times 2.2$ lower than in SN 1987A, while the ^{56}Ni masses are similar. We therefore deduce an oxygen mass of about one half of that found in SN 1987A, i.e. $\sim 0.7\text{--}1.0 M_{\odot}$ in SN 2002hh. This suggests a massive progenitor with a main-sequence stellar mass of 16–18 M_{\odot} (Woosley & Weaver 1995), somewhat less than the 20 M_{\odot} of SN 1987A. Within the context of the Thielemann et al. models, this would be consistent with the observed lower silicon mass and possibly also with the lower calcium abundance in SN 2002hh. However, the apparent conflict with the strong Mg I 1.503 μm luminosity remains.

A striking difference between SN 1987A and SN 2002hh lies in the velocity shifts of some of the more prominent, isolated lines. While blueshifts of order -500 km s^{-1} were seen in SN 2002hh, *redshifts* of about the same size were seen in the same lines and phases in SN 1987A. These shifts were discussed in Spyromilio et al. (1990) and Meikle et al. (1993). It was concluded that asymmetry in the ejecta was the most likely explanation. As indicated above, we propose that the blueshifts in SN 2002hh have a similar origin.

As already mentioned, during the first year of SN 2002hh we find no line profile-based evidence of dust condensation in the ejecta. This is consistent with an SN 1987A-like behaviour, where the first sign of dust condensation was at about 1 year (Meikle et al. 1993) and substantial dust-induced line attenuation did not occur until about 500–530 days (Danziger et al. 1991). The clear presence of CO emission by 200 d indicates that conditions may eventually allow grain condensation. However, the CO emission was generally weaker than seen in SN 1987A and so the mass of condensing dust may be less. Nevertheless, Meikle et al. (2005a,b and in prep.) report mid-IR evidence for the condensation of $\sim 10^{-3} M_{\odot}$ of dust by day 590 - a very similar mass and condensation epoch to those of SN 1987A. Modelling of the CO first-overtone emission using the constraint of the ^{56}Ni mass derived from the bolometric light-curve, might provide an additional constraint on the progenitor core mass as was done for SN 1998S by Fassia et al. (2001). However, this is beyond the scope of this paper.

Based on the IR-echo interpretation of the late-time *KL* excess we deduce that the progenitor of SN 2002hh underwent a mass-loss of $\sim 0.3 M_{\odot}$. This is similar to the CSM mass derived for the Type IIL SN 1980K by Dwek (1983), also based on IR-echo analysis. While this may be less than that of SN 1987A (e.g. Sugerman et al. 2005), the strong and relatively early IR excess points to a substantial proportion lying within ~ 100 light-days of the supernova - much closer

than for SN 1987A. Likewise, the strong radio luminosity of SN 2002hh (Beswick et al. 2005) as early as 381 d points to recent substantial mass-loss. Indeed, the radio luminosities reported by Beswick et al. are very similar to those of SN 1980K from which Weiler et al. (1992) derived a CSM mass exceeding $0.34 M_{\odot}$. However, we do not find evidence for the enormously massive (10–15 M_{\odot}) CSM claimed by Barlow et al. (2005). Extrapolating our IR echo model to the earliest epoch of the Spitzer Space Telescope observations *viz.* 590 days, it predicts a flux of $\sim 0.4 \text{ mJy}$ at 5.8 μm and 8.0 μm . This is 10 per cent or less of the fluxes quoted by Barlow et al. Furthermore, a mass loss of 10–15 M_{\odot} is about 100 times larger than the value recently estimated by Chevalier, Fransson & Nymark (2005) by modelling the radio data of Chandra et al. (2003) and Stockdale et al. (2004).

Given that the progenitor was probably massive and that the light curves exhibit a significant plateau phase, we conclude that the progenitor of SN 2002hh was a red supergiant as expected for normal type IIP SNe (see Popov 1993; see also Li et al. 2005b and references therein). There is also evidence that a substantial, dusty wind was emitted by the progenitor star and that the mass outflow was ongoing almost up to the epoch of explosion. However, in spite of the progenitor differences between SN 2002hh and SN 1987A, much of their nebular spectroscopic behaviour was remarkably similar.

ACKNOWLEDGMENTS

We would like to thank R. Stathakis for having provided us with the SN 1987A optical spectra in digitized format. Thanks also to M. Gustafsson, P. Jakobsson, J. Melinder and G. Øye for observing and reducing the NOT spectrum of SN 2002hh; and to R. Chornock, S. Jha, M. Papenkova, B. Swift and D. Weisz for observing the Lick and Keck/ESI SN 2002hh spectra. This work is based on observations collected at the William Herschel Telescope (WHT), La Palma, the Nordic Optical Telescope (NOT), La Palma, the Infrared Telescope Facility (IRTF), Hawaii, the Keck Telescope, Hawaii and the Shane Telescope at Lick Observatory, CA. The WHT is operated on the island of La Palma by the Isaac Newton Group (ING) in the Spanish Observatorio del Roque de los Muchachos of the Instituto de Astrofísica de Canarias. The NOT is operated on the island of La Palma jointly by Denmark, Finland, Iceland, Norway, and Sweden, in the Spanish Observatorio del Roque de los Muchachos of the Instituto de Astrofísica de Canarias. IRTF is operated on behalf of NASA by the University of Hawaii. Keck Observatory is operated by the California Association for Research in Astronomy (CARA). Lick Observatory is operated by the University of California. MP is supported through PPARC grant PPA/G/S/2001/00512.

REFERENCES

- Arnett W.D., Fu A., 1989, ApJ, 340, 396
- Barlow M., Fabbri J., Meixner M., Sugerman B., 2004, IAU Circ. 8400
- Barlow M.J., et al., 2005, ApJ, 627, L113

- Baron E., et al., 2000, *ApJ* 545, 444
- Bersanelli M., Bouchet P., Falomo R., 1991, *A&A*, 252, 854
- Bessell M.S., 1979, *PASP*, 91, 589
- Bessell M.S., 1999, *PASP*, 111, 1426
- Beswick R.J., Fenech D., Thrall H., Argo M.K., Muxlow T.W.B., Pedlar A., 2005, *IAU Circ.* 8572
- Bode M.F., Evans A., 1980, *MNRAS*, 193, 21
- Bohlin R.C., Savage B.D., Drake J.F., 1978, *ApJ*, 224, 132
- Bonnarel F., Boulesteix J., Marcelin M., 1986, *A&A*, 66, 149
- Bouchet P., Danziger I.J., 1993, *A&A*, 273, 45
- Bouchet P., Danziger I.J., Lucy L.B., 1991, *AJ*, 102, 1135
- Bouchet P., Slezak E., Le Bertre T., Moneti A., Manfroid J., 1989, *A&AS*, 80, 379
- Cardelli J.A., Clayton G.C., Mathis J.S., 1989, *ApJ*, 345, 245
- Catchpole R.M. et al., 1987, *MNRAS*, 229, 15
- Catchpole R.M. et al., 1988, *MNRAS*, 231, 75
- Cernuschi F., Marsicano F., Codina S., 1967, *Ann. d'Astr.*, 30, 1039
- Chandra P., Ray A., Bhatnagar S., 2003, *IAU Circ.* 8041
- Chevalier R.A., Fransson C., Nymark T.K., 2005, *ApJ*, in press (astro-ph/0509468).
- Danziger I.J., Lucy L.B., Bouchet P., Gouiffes C., 1991, in *Supernovae. The Tenth Santa Cruz Workshop in Astronomy and Astrophysics*, July 9-21, 1989, Lick Observatory. S.E. Woosley editor, Springer-Verlag, New York, p. 69
- Dessart L., Hillier D.J., 2005, *A&A*, 437, 667
- Draper P.W., Gray N., Berry D.S., 2002, *Starlink User Note* 214.10
- Dunne L., Eales S., Ivison R., Morgan H., Edmunds M., 2003, *Nat*, 424, 285
- Dwek E., 1983, *ApJ*, 274, 175
- Dwek E., 1985, *ApJ*, 297, 719
- Dwek E., 1998, *ApJ*, 501, 643
- Elmhamdi A. et al., 2003, *MNRAS*, 338, 939
- Fassia A., Meikle W.P.S., 1999, *MNRAS*, 302, 314
- Fassia A., Meikle W.P.S., Geballe T.R., Walton N.A., Pollacco D.L., Rutten R.G.M., Tinney C., 1998, *MNRAS*, 299, 150
- Fassia A. et al. 2001, *MNRAS*, 325, 907
- Fassia A., Meikle W.P.S., Spyromilio J., 2002, *MNRAS*, 332, 296
- Filippenko A.V., 1982, *PASP*, 94, 715
- Filippenko A.V., Foley R.J., Swift B., 2002, *IAU Circ.* 8007
- Filippenko A. V., Li W.D., Treffers R.R., Modjaz M., 2001, in *IAU Colloq. 183, Small Telescope Astronomy on Global Scales*, ed. W.-P. Chen, C. Lemme, and B. Paczyński (ASP Conf. Ser. 246; San Francisco: ASP), 121
- Gearhart R.A., Wheeler J.C., Swartz D.A., 1999, *ApJ*, 510, 944
- Gehrz R., 1989, in *Interstellar Dust: Proceedings of the 135th Symposium of the International Astronomical Union*, 26-30 July, 1988, Santa Clara, California. L.J. Allamandola and A.G.G.M. Tielens editors, Kluwer, Dordrecht, p. 445
- Gerardy C.L., Fesen R.A., Höflich P., Wheeler J.C., 2000, *AJ*, 119, 2968
- Gerardy C.L., Fesen R.A., Nomoto K., Maeda K., Höflich P., Wheeler C., 2002, *PASJ*, 54, 905
- Graham J.R., 1988, *ApJ*, 335, L53
- Graham J.R., Meikle W.P.S., 1986, *MNRAS*, 221, 789
- Hamuy M., Suntzeff N.B., Gonzales R., Martin G., 1988, *AJ*, 95, 63
- Hamuy et al., 2001, *ApJ*, 558, 615
- Holwerda B.W., Gonzalez R.A., Allen R.J., van der Kruit P.C., 2005, *AJ*, 129, 1396
- Horne K., 1986, *PASP*, 98, 609
- Hoyle F., Wickramasinghe N.C., 1970, *Nat*, 226, 62
- Karachentsev I.D., Sharina M.E., Huchtmeier W.K., 2000, *A&A*, 362, 544
- Kotak R., Meikle W.P.S., Adamson A., Leggett S.K., 2004, *MNRAS*, 354, L13
- Krause O., Birkmann S.M., Rieke G.H., Lemke D., Klaas U., Hines D.C., Gordon K.D., 2004, *Nat*, 432, 596
- Leonard D.C. et al. 2002a, *PASP*, 114, 35
- Leonard D.C. et al. 2002b, *AJ*, 124, 2490
- Leonard D.C., Kanbur S.M., Ngeow C.C., Tanvir N.R., 2003, *ApJ*, 594, 247
- Li W., 2002, *IAU Circ.* 8005
- Li W. et al. 2000, in *Cosmic Explosions*, ed. S.S. Holt and W.W. Zhang (New York: AIP), 103
- Li W. et al., 2001, *PASP*, 113, 1178
- Li W., Van Dyk S.D., Filippenko A.V., Cuillandre J.-C., 2005a, *PASP*, 117, 121
- Li W., Van Dyk S.D., Filippenko A.V., Cuillandre J.-C., Jha S., Bloom J.S., Riess A.G., Livio M., 2005b, *ApJ*, in press (astro-ph/0507394).
- Liu W., Dalgarno A., 1995, *ApJ*, 454, 472
- Lucy L.B., Danziger I.J., Gouiffes C., Bouchet P., 1991, in *Supernovae. The Tenth Santa Cruz Workshop in Astronomy and Astrophysics*, July 9-21, 1989, Lick Observatory. S.E. Woosley editor, Springer-Verlag, New York, p. 82
- Martos M., Hernandez X., Yáñez M., Moreno E., Pichardo B., 2004, *MNRAS*, 350, L47
- Matheson T. et al., 2000a, *AJ*, 120, 1487
- Matheson T., Filippenko A.V., Ho L.C., Barth A.J., Leonard D.C., 2000b, *AJ*, 120, 1499
- Mattila S., Meikle W.P.S., 2001, *MNRAS*, 324, 325
- Meikle W.P.S., Allen D.A., Spyromilio J., Varani G.-F., 1989, *MNRAS*, 238, 193
- Meikle W.P.S., Spyromilio J., Allen D.A., Varani G.-F., Cumming R.J., 1993, *MNRAS*, 261, 535
- Meikle P., Mattila S., Smartt S., MacDonald E., Clewley L., 2002, *IAU Circ.* 8024
- Meikle P., Fassia A., Geballe T.R., Lundqvist P., Chugai N., Farrah D., Sollerman J., 2003, in *From Twilight to Highlight: The Physics of Supernovae*, Proceedings of the ESO/MPA/MPE Workshop, Garching, Germany, 29-31 July 2002, p.229
- Meikle W.P.S., 2005a, Invited talk given at the National Astronomy Meeting, Birmingham, 2005 April 4-8
- Meikle W.P.S., 2005b, Invited talk given at the 206th American Astronomical Society Meeting, Minneapolis, 2005 May 29 - June 2, 28.09
- Miller S., Tennyson J., Lepp S., Dalgarno A., 1992, *Nat*, 355, 420
- Miller J. S., Stone R.P.S., 1993, *Lick Obs. Tech. Rep. No. 66* (Santa Cruz, CA: Lick Obs.)
- Milne P.A., Wells L.A., 2003, *AJ*, 125, 181
- Munari U., Zwitter T., 1997, *A&A*, 318, 269
- Nozawa T., Kozasa T., Umeda H., Maeda K., Nomoto K., 2003, *ApJ*, 598, 785
- Oke J.B. et al., 1995, *PASP*, 107, 375
- Patat F., 2005, *MNRAS*, 357, 1161
- Pooley D., Lewin W.H.G., 2002, *IAU Circ.* 8024
- Popov D.V., 1993, *ApJ*, 414, 712
- Pozzo M., Meikle W.P.S., Fassia A., Geballe T., Lundqvist P., Chugai N.N., Sollerman J., 2004, *MNRAS*, 352, 457
- Press W. H., Teukolsky S. A., Vetterling W. T., Flannery B. P., 1992, *Numerical Recipes*, 2nd edn. Cambridge University Press, Cambridge
- Rayner J.T., Toomey D.W., Onaka P.M., Denault A.J., Stahlberger W.E., Vacca W.D., Cushing M.C., Wang S., 2003, *PASP*, 115, 362
- Romaniello M., Salari M., Cassisi S., Panagia N., 2000, *ApJ*, 530, 738
- Romaniello M., Panagia N., Scuderi S., Kirshner R.P., 2002, *AJ*, 123, 915
- Schlegel D.J., Finkbeiner D.P., Davis M., 1998, *ApJ*, 500, 525
- Sheinis A.I., Bolte M., Epps H.W., Kibrick R.I., Miller J.S., Radovan M.V., Bigelow B.C., Sutin B.M., 2002, *PASP*, 114, 851

- Shortridge K., 1991, FIGARO General Data Reduction and Analysis Starlink MUD, RAL, June 1991
- Spyromilio J., Leibundgut B., 1996, MNRAS, 283, L89
- Spyromilio J., Meikle W.P.S., Learner R.C.M., Allen D.A., 1988, Nat, 334, 327
- Spyromilio J., Meikle W.P.S., Learner R.C.M., Allen D.A., 1989, in Kaldeich B.H., ed., 22nd ESLAB Symp. on Infrared Spectroscopy in Astronomy. ESA Publications Division, ESTEC, Noordwijk, p. 381
- Spyromilio J., Meikle W.P.S., Allen D.A., 1990, MNRAS, 242, 669
- Spyromilio J., Stathakis R.A., Cannon R.D., Waterman L., Couch W.J., Dopita M.A., 1991, MNRAS, 248, 465
- Spyromilio J., Stathakis R.A., Meurer G.R., 1993, MNRAS, 263, 530
- Spyromilio J., Leibundgut B., Gilmozzi R., 2001, A&A, 376, 188
- Stathakis R.A., 1996, PhD Thesis University of Sydney
- Stockdale C.J., et al., 2002, IAU Circ. 8018
- Stockdale C.J., Sramek R.A., Rupen M., Weiler K.W., Van Dyk S.D., Panagia N., 2004, <http://rsd-www.nrl.navy.mil/7213/weiler/kwdata/02hhdata.asc>
- Sugerman B., Barlow M., Fabbri J., Meixner M., 2005, in the 205th AAS Meeting, San Diego, CA, 9-13 Jan. 2005
- Suntzeff N.B., Hamuy M., Martin G., Gomez A., Gonzales R., 1988, AJ, 96, 1864
- Thielemann F.-K., Nomoto K., Hashimoto M.-A., 1996, ApJ, 460, 408
- Tielens A.G.G.M., 1990, in Submillimetre Astronomy. Watt G.D., Webster A.S., editors, Kluwer, Dordrecht, p.13
- Todini P., Ferrara A., 2001, MNRAS, 325, 726
- Varani G.-F., Meikle W.P.S., Spyromilio J., Allen D.A., 1990, MNRAS, 245, 570
- Wang J., Hall P.B., Ge J., Li A., Schneider D.P., 2004, ApJ, 609, 589
- Weiler K.W., van Dyk S.D., Panagia N., Sramek R.A., 1992, ApJ, 398, 248
- Whitelock P.A. et al., 1988, MNRAS, 234, 5
- Wooden D.H., 1989, PhD Thesis, Univ. California, Santa Cruz
- Wooden D.H., Rank D.M., Bregman J.D., Witteborn F.C., Tielens A.G.G.M., Cohen M., Pinto P.A., Axelrod T.S., 1993, ApJS, 88, 477
- Wooden D.H., 1997, in Infrared Space Interferometry : Astrophysics & the Study of Earth-Like Planets. C. Eiroa et al. eds., Kluwer, Dordrecht, p.133
- Woosley S.E., 1988, ApJ, 330, 218
- Woosley S.E., Weaver T.A., 1995, ApJS, 101, 181

This paper has been produced using the Royal Astronomical Society/Blackwell Science L^AT_EX style file.